Bioorganic Chemistry 85 (2019) 1–17

Contents lists available at ScienceDirect

Bioorganic Chemistry

journal homepage: www.elsevier.com/locate/bioorg

Syntheses and evaluation of new Quinoline derivatives for inhibition of hnRNP K in regulating oncogene *c-myc* transcription

Bing Shu[a,b], Ping Zeng[a], Shuangshuang Kang[a], Peng-Hui Li[a], Dexuan Hu[a], Guotao Kuang[a], Jiaojiao Cao[a], Xiaoya Li[a], Meiling Zhang[a], Lin-Kun An[a], Zhi-Shu Huang[a], Ding Li[a,*]

[a] School of Pharmaceutical Sciences, Sun Yat-sen University, Guangzhou University City, 132 Waihuan East Road, Guangzhou 510006, PR China
[b] School of Pharmacy, Guangdong Pharmaceutical University, Guangzhou 510006, PR China

ARTICLE INFO

Keywords:
hnRNP K
c-myc
Quinoline
i-motif
Cancer

ABSTRACT

Aberrant overexpression of heterogeneous nuclear ribonucleoprotein K (hnRNP K) is a key feature in oncogenesis and progression of many human cancers. hnRNP K has been found to be a transcriptional activator to up-regulate *c-myc* gene transcription, a critical proto-oncogene for regulation of cell growth and differentiation. Therefore, down-regulation of *c-myc* transcription by inhibiting hnRNP K through disrupting its binding to *c-myc* gene promoter is a potential approach for cancer therapy. In the present study, we synthesized and screened a series of Quinoline derivatives and evaluated their binding affinity for hnRNP K. Among these derivatives, (*E*)-1-(4-methoxyphenyl)-3-(4-morpholino-6-nitroquinolin-2-yl)prop-2-en-1-one (compound **25**) was determined to be the first-reported hnRNP K binding ligand with its K_D values of 4.6 and 2.6 μM measured with SPR and MST, respectively. Subsequent evaluation showed that the binding of compound **25** to hnRNP K could disrupt its unfolding of *c-myc* promoter i-motif, resulting in down-regulation of *c-myc* transcription. Compound **25** showed a selective anti-proliferative effect on human cancer cell lines with IC_{50} values ranged from 1.36 to 3.59 μM. Compound **25** exhibited good tumor growth inhibition in a Hela xenograft tumor model, which might be related to its binding with hnRNP K. These findings illustrated that inhibition of DNA-binding protein hnRNP K by compound **25** could be a new and selective strategy of regulating oncogene transcription instead of targeting promoter DNA secondary structures such as G-quadruplexes or i-motifs.

1. Introduction

The human *c-myc* protogene is an important regulator of a wide array of cellular processes necessary for normal cell growth and differentiation, and its dysregulation is one of the hallmarks of many cancers [1–3]. The aberrant overexpression of this gene is closely related to the occurrence and development of various human cancers [4]. Therefore, the strategy of suppressing *c-myc* transcription and expression in established cancer cell lines has been investigated extensively [5–7]. It has been shown that the crystal structure of c-MYC protein does not have an apparent ligand-binding cavity, which make it difficult to design protein-binding ligands [8,9], and therefore it becomes important to modulate *c-myc* transcription through *c-myc* gene promoter. The G-quadruplex and i-motif formed in GC-rich region of *c-myc* gene promoter have been shown to suppress *c-myc* gene transcription, and a variety of ligands binding to and stabilizing these DNA secondary structures can regulate gene transcription [10–14]. However, due to overwhelming abundance of these types of DNA secondary structures in genomic sequence, the selective targeting by small molecule ligands is a problem. Therefore, development of a new and more selective strategy of regulating oncogene transcription instead of targeting widely existed DNA secondary structures such as G-quadruplexes and i-motifs has become more and more important.

Heterogeneous nuclear ribonucleo protein K (hnRNP K) encodes a multifunctional transcription factor [15–17] that plays a critical role in a broad range of cellular processes, including the regulation of cell cycle progression, cell growth, differentiation, transformation, angiogenesis, and apoptosis [15,18,19]. Besides, hnRNP K has been suggested to be related with other transcription factors such as heat shock proteins [20]. It has been shown that the overexpression of hnRNP K is associated with development of chronic myeloid leukemia, prostate, colorectal and breast cancer possibly through activation of *c-myc* gene, indicating hnRNP K as a potential drug target for cancer treatment [21]. The previous investigations have implicated that hnRNP K could up-regulate *c-myc* gene transcription through its binding interaction with C-rich sequence of *c-myc* gene promoter [16,22]. It has been reported

* Corresponding author.
E-mail address: liding@mail.sysu.edu.cn (D. Li).

https://doi.org/10.1016/j.bioorg.2018.12.020
Received 22 October 2018; Received in revised form 13 December 2018; Accepted 14 December 2018
Available online 22 December 2018
0045-2068/

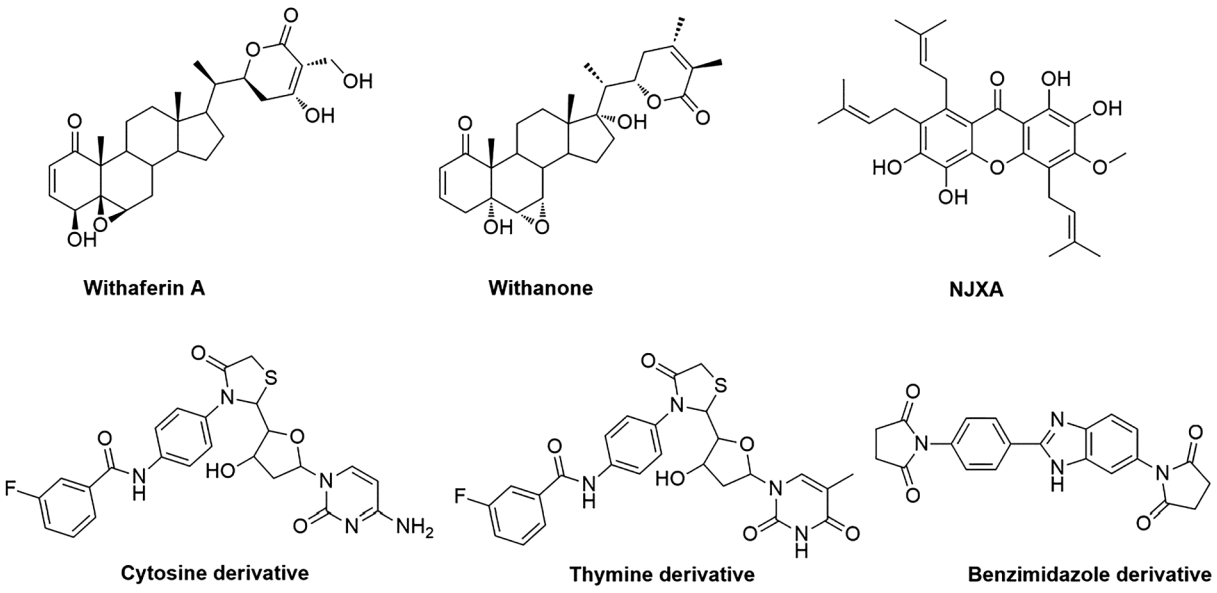

Fig. 1. The structures of **Withaferin A**, **Withanone**, **NJXA**, **Cytosine derivative**, **Thymine derivative,** and **Benzimidazole derivative**.

that hnRNP K could recognize and bind to the 3′ lateral and central loops of the i-motif in the promoter of *c-myc* gene leading to transcriptional activation [23,24]. Dash *et al* have reported that **PBP1** could induce the formation of *c-myc* promoter i-motif resulting in down-regulation of *c-myc* luciferase expression [14]. Recently, we have reported that acridone **B19** could induce the formation of *c-myc* promoter i-motif selectively without significant effect on its corresponding G-quadruplex resulting in down-regulation of *c-myc* transcription [13]. The existence of i-motifs in cells has recently been demonstrated by using antibodies, which might play important roles as transcriptional regulators [25–27]. The above findings indicated that hnRNP K could bind to oncogene promoter i-motifs and act as transcriptional activator. Hence, disruption of the hnRNP K/i-motif interaction through specific binding of small molecules to hnRNP K could provide a new and selective method for down-regulating oncogene transcription instead of targeting widely-existed gene promoter i-motif structures in cells [6,7,28].

It has been reported that Withanone and Withaferin A (Fig. 1) could inhibit cancer cells growth, migration, angiogenesis and metastasis through targeting hnRNP K [29]. The unsaturated ketones seem to be the pharmacophores, however the mechanism is uncertain with only MD simulations. Xu group have reported that Nujiangexathone A (NJXA) could reduce the expression of hnRNP K by accelerating ubiquitin-proteasome-dependent hnRNP K degradation [30], however NJXA did not interact with hnRNP K directly. Several other ligands have been designed based on the KH3 domain of hnRNP K, such as cytosine derivative, thymine derivatives, and benzimidazole derivatives. These structures also contain the unsaturated ketones or similar bioisosteres (Fig. 1) [21,31], however these compounds have not been shown to interact with hnRNP K. Therefore, discovery and development of highly selective hnRNP K binding ligands are important to gain new insight for hnRNP K regulated oncogene transcription.

In this study, we overexpressed and purified hnRNP K, which was able to bind with C-rich sequence/i-motif of *c-myc* gene promoter. Then we screened our synthesized compounds library in our laboratory (110 compounds, including acridone derivatives, quinoline derivatives, acridine derivatives, imidazole derivatives, and indole derivatives, Fig. S1) by using SPR. Among these compounds, we identified a Quinoline derivative, (*E*)-1-(4-chlorophenyl)-3-(6-methoxy-4-morpholinoquinolin-2-yl)prop-2-en-1-one (compound **Q16**, Fig. S1), with the binding affinity IC_{50} value of 20.1 μM as a hit compound. In order to obtain stronger hnRNP K binding ligands and study the structure-activity relationship, we designed and synthesized a series of Quinoline derivatives (**07**–**37**) with various substitutive groups (Fig. S2). Then the binding affinity of these compounds for hnRNP K was evaluated, and (*E*)-1-(4-methoxyphenyl)-3-(4-morpholino-6-nitroquinolin-2-yl)prop-2-en-1-one (compound **25**) was found to bind tightly to hnRNP K. Our further *in vitro* and cellular experiments suggested that compound **25** as the first determined hnRNP K binding ligand could bind to hnRNP K and disrupt the interaction between hnRNP K and *c-myc* gene promoter i-motif. This caused down-regulation of *c-myc* transcription and translation, resulting in tumor cells proliferation inhibition and apoptosis. These results could provide a new and selective strategy of regulating oncogene transcription instead of targeting DNA secondary structures such as G-quadruplexes or i-motifs.

2. Results and discussion

2.1. Chemistry

The synthetic pathway for Quinoline derivatives **07**–**37** was shown in Scheme 1. 4-Substituted anilines (**1a–d**) were used as the starting materials to react with ethyl acetoacetate to give 2-methyl-6-substituted-quinolin-4-ol (**2a–d**), which were then reacted with phosphorus oxychloride immediately to generate Quinoline derivatives **3a–d**. Quinoline derivatives **4a–d** were prepared through reaction of **3a–d** with Morpholine solution catalyzed with Ts-OH. The products were used directly for the next step reaction without purification. Compounds **4a–d** reacted with selenium dioxide through Riley oxidation reaction to give key compounds **5a–d**. Finally, the target Quinoline derivatives **07**–**37** were obtained through aldol reaction between aldehyde **5a–d** and 1-(4-substituted phenyl)ethanone (**6a-f**) catalyzed with H_2SO_4 in AcOH solution or in EtOH solution containing 10% NaOH. Under various reaction conditions, we obtained Quinoline derivatives with hydroxyl substitutive group (**31**–**33**). Compound **5b** reacted with 3-morpholinopropan-1-amine to give a propylamine derivative (**34**). Methylation derivative **35** was obtained with compound **07** as the starting material stirred in methyl iodide solution. Lastly, compound **12** was reduced under hydrogen atmosphere to give derivatives **36**–**37**. The synthesized Quinoline derivatives were purified, and their structures were determined by using HPLC, NMR and high resolution mass spectra.

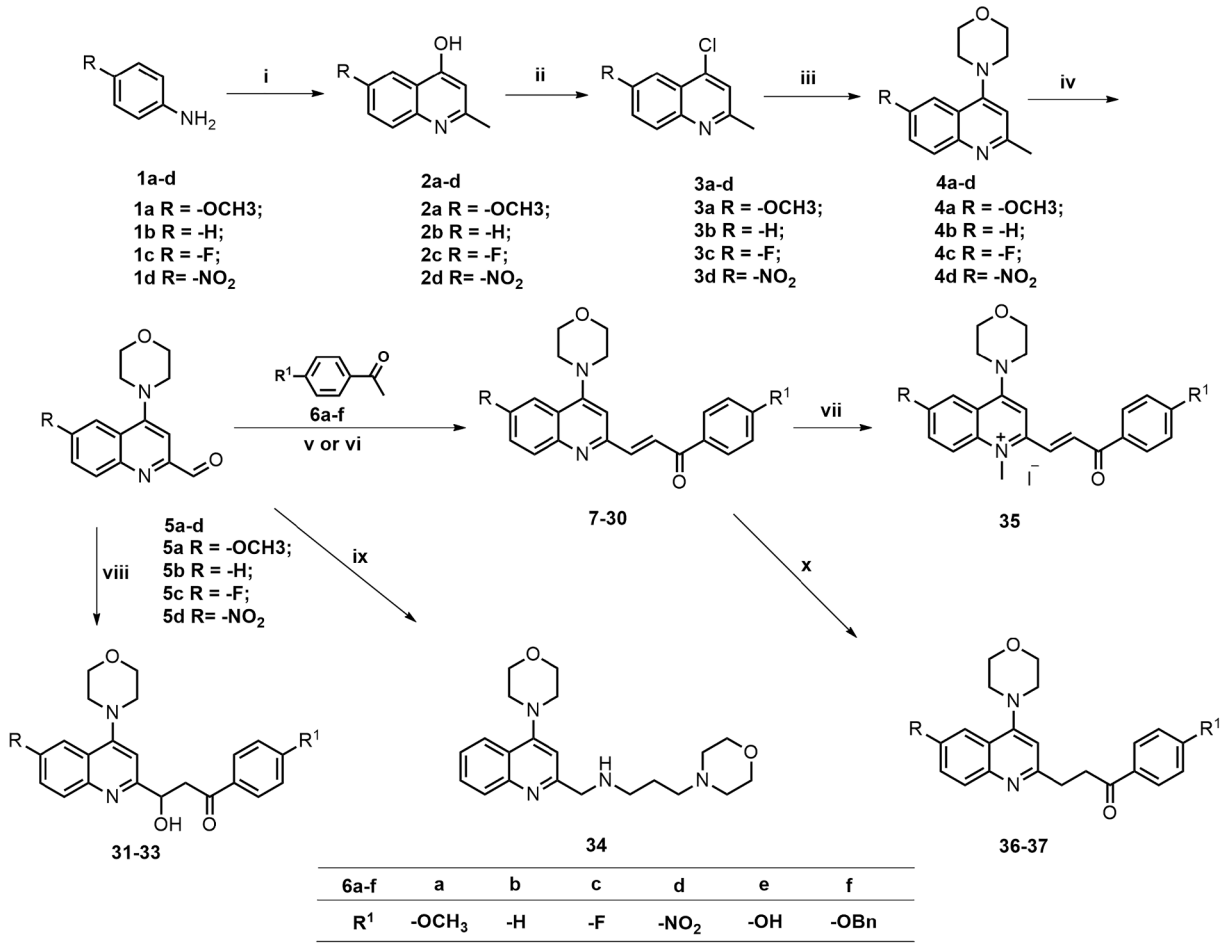

Scheme 1. Reagents and conditions: (i) PPA, 120 °C, 12 h; (ii) $POCl_3$, 100 °C, 4 h, yield 45–57% for two steps; (iii) Morpholine, TsOH, 120 °C, 1 h, yield 75–82%; (iv) 1,4-dioxane, SeO_2, 80 °C, 2 h, yield 61–78%; (v) acetophenones (**6a–e**), HAc, H_2SO_4, 10 h, yield 30–75%; (vi) 1-(4-(benzyloxy)phenyl)ethanone (**6f**), 10% NaOH solution, EtOH, 5 °C, yield 64–79%; (vii) CH_3I, THF, 70 °C, 2 days, yield 35%; (viii) EtOH, 1% NaOH, r.t., yield 70–84%; (ix) 3-morpholinopropan-1-amine, $NaBH_3CN$, TCM, HAc, r.t., overnight, yield 43%; (x) ethyl acetate, 5% Pd/C, H_2, r.t., yield 35–41%.

2.2. Cloning, overexpression in E. coli, purification and characterization of hnRNP K

hnRNP K has been cloned, overexpressed in *E. coli* and purified by using affinity chromatography methods, which has been identified by using SDS gel electrophoresis as described previously [32,33]. In the present study, hnRNP K was purified to apparent homogeneity based on SDS–PAGE as shown in Fig. S3a, which was confirmed by using Western blot as shown in Fig. S3b. It has been previously reported that hnRNP K specifically bound to a single-stranded *cis*-element comprised of five imperfect CCCT repeats (CCCTCCCCA) [34]. To confirm the binding activity of our purified hnRNP K protein, electrophoretic mobility shift assay (EMSA) was used to study the interaction between hnRNP K and single-stranded CCCT repeat DNA. As shown in Fig. S3c, when increasing the concentration of hnRNP K in a mixture of protein and single-stranded CCCT repeat DNA, the concentration of protein-bound DNA increased, which was consistent with that reported previously [35], and indicated that the purified hnRNP K was good enough for further biophysical and biochemical studies.

2.3. hnRNP K could unfold the i-motif of c-myc NHE III_1

The nuclease hypersensitive element III_1 (NHE III_1), located at upstream from the P1 promoter of *c-myc* gene, has controlled 85–90% of *c-myc* transcription [4,10]. As mentioned above, hnRNP K selectively bound to single-stranded CCCT repeat DNA. There is convincing evidence that this protein has an important role in the control of *c-myc* gene expression through binding to the C-rich strand of DNA [36]. In the present study, we used a 33-bp single strand DNA (Table S1) probe in *c-myc* NHE III_1 domain, containing repeats of known hnRNP K

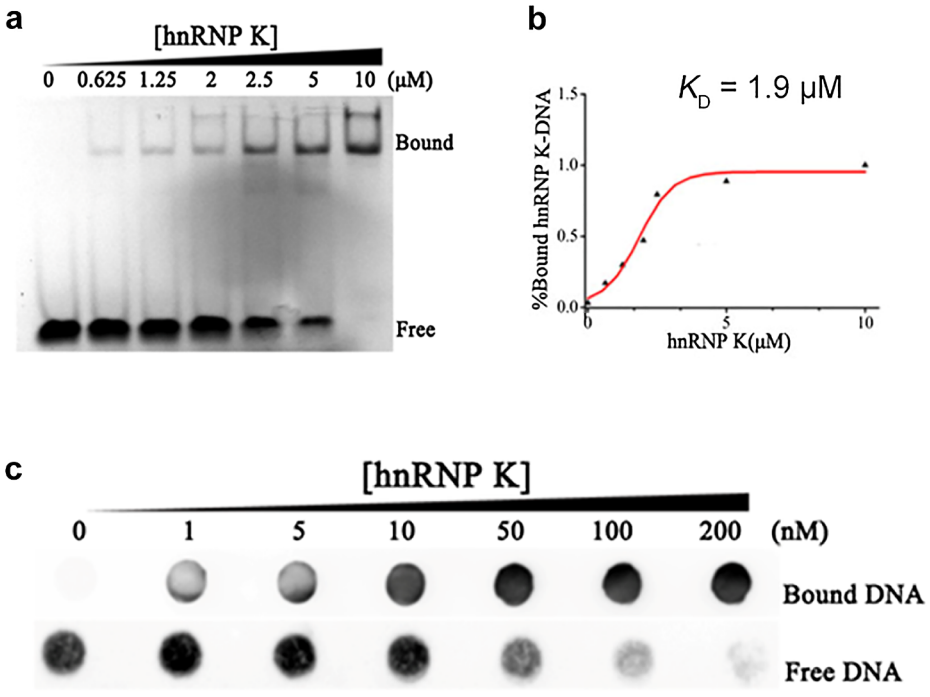

Fig. 2. The interaction of hnRNP K with *c-myc* promoter C-rich DNA. (a) The binding of hnRNP K with *c-myc* Py33 analyzed by using EMSA; (b) Binding curve for determination of the binding constant for the interaction between hnRNP K and *c-myc* Py33 based on EMSA data; (c) Filter binding assay for the interaction of hnRNP K with *c-myc* Py33.

Table 1
Binding affinity of the Quinoline derivatives to hnRNP K protein determined by using SPR.

Comp.	R	R^1	K_D (μM)	Comp.	R	R^1	K_D (μM)
7	$-OCH_3$	$-OCH_3$	7.2	**23**	-F	-OH	11.6
8	$-OCH_3$	-H	11.6	**24**	-F	-OBn	9.8
9	$-OCH_3$	-F	15.3	**25**	$-NO_2$	$-OCH_3$	4.6
10	$-OCH_3$	$-NO_2$	> 30[a]	**26**	$-NO_2$	-H	23.7
11	$-OCH_3$	-OH	23.2	**27**	$-NO_2$	-F	11.3
12	$-OCH_3$	-OBn	14.2	**28**	$-NO_2$	$-NO_2$	> 30
13	-H	$-OCH_3$	9.7	**29**	$-NO_2$	-OH	7.1
14	-H	-H	23.1	**30**	$-NO_2$	-OBn	13.2
15	-H	-F	15.0	**31**	$-OCH_3$	$-NO_2$	> 30
16	-H	$-NO_2$	> 30	**32**	$-OCH_3$	-OBn	> 30
17	-H	-OH	6.7	**33**	-H	-OBn	> 30
18	-H	-OBn	14.2	**34**	-	-	23.1
19	-F	$-OCH_3$	6.8	**35**	$-OCH_3$	$-OCH_3$	16.7
20	-F	-H	10.5	**36**	$-OCH_3$	-OH	> 30
21	-F	-F	27.1	**37**	$-OCH_3$	-OBn	> 30
22	-F	$-NO_2$	> 30	**Q16**			20.1

[a] No significant binding was detected upon addition of up to 30 μM ligand, which might indicate no specific interaction between the ligand and the protein.

recognition motif (5′-dTCCC) with a single fluorescent dye labeled to the 5′-end of the forward strand [34]. Previously, the hnRNP K KH_3 domain has been identified as the minimal component of the canonical hnRNP-K-DNA binding mode [37]. The dissociation equilibrium constant for the KH_3 form of the protein to its 30 bp DNA (5′-CTCTCCTT TCTTTTTCTTCTTCCCTCCCTA-3′) calculated from a steady state analysis has been determined to be K_D = 1.5 μM by using SPR experiment [35]. In our present study, EMSA was used to determine the binding between the full length hnRNP K and the *c-myc* DNA probe. Our result showed that the hnRNP K associated with the DNA probe in a dose-dependent manner with K_D of 1.9 μM as shown in Fig. 2a and b, which was consistent with that reported previously. This result was also supported by the data from our filter binding assay. As shown in Fig. 2c, when increasing the concentration of hnRNP K, the protein-bound DNA was also increased. Besides, it has been shown that C-rich strand in *c-myc* promoter could form an i-motif structure and affect gene transcription [38,39]. However, it was not clear whether hnRNP K could interact with *c-myc* promoter i-motif or not. In the present research, we studied the interaction of hnRNP K with *c-myc* promoter i-motif through circular dichroism (CD) spectroscopy and fluorescence resonance energy transfer (FRET). The CD spectrum of Py33 sequence showed a positive peak near 288 nm and a negative peak near 260 nm in a buffer at pH 6.0, indicating the formation of i-motif structure, as shown in Fig. S4a. After one equivalent of hnRNP K was added, the above two peaks were both decreased with the peak at 288 nm shifted toward 276 nm, which were similar to those reported previously by Qu group and Hurley group, indicating that hnRNP K could unfold the i-motif into an unordered random coil [40–43]. The unwinding activity of hnRNP K for i-motif was also confirmed by using FRET assay, as shown in Fig. S4b. The fluorescence intensity at 580 nm was decreased upon addition of increasing concentration of hnRNP K. All above results showed that our hnRNP K could unfold the *c-myc* promoter i-motif into an unordered random coil in a dose-dependent manner, which could be further used for screening of protein inhibitors.

2.4. Binding studies of the Quinoline derivatives for hnRNP K

The binding affinities of the synthesized compounds for the hnRNP K were studied through surface plasmon resonance (SPR) experiments [44,45], and the dissociation constants (K_D) were determined as shown in Table 1. Quinoline derivatives (**07–30**) showed good binding affinity for hnRNP K, especially the derivatives with resonance electron donating R^1 substitutive groups, such as $-OCH_3$, -H, -F, -OH, and –OBn (compounds **7–9**, **11–15**, **17–21**, **23–27**, and **29–30**), had their K_D values ranged from 4.6 to 25.7 μM. In contrast, the derivatives with resonance electron withdrawing R^1 substitutive groups, such as $-NO_2$ (compounds **10**, **16**, **22**, and **28**), showed no significant binding with hnRNP K upon addition of up to 30 μM ligands. In comparison, R substitutive groups seem to have less significant effect on the binding affinity. The compounds **7**, **13**, **19**, and **25**, with R substitutive groups of $-OCH_3$, -H, -F, and $-NO_2$, had their K_D values of 7.2, 9.7, 6.8, and 4.6, respectively. These results indicated that R^1 substituent is important to maintain the binding affinity. We also modified the unsaturated ketone in the middle of Quinoline derivatives to generate hydroxylation derivatives (**31–33**), propylamine derivative (**34**), and reduced derivatives

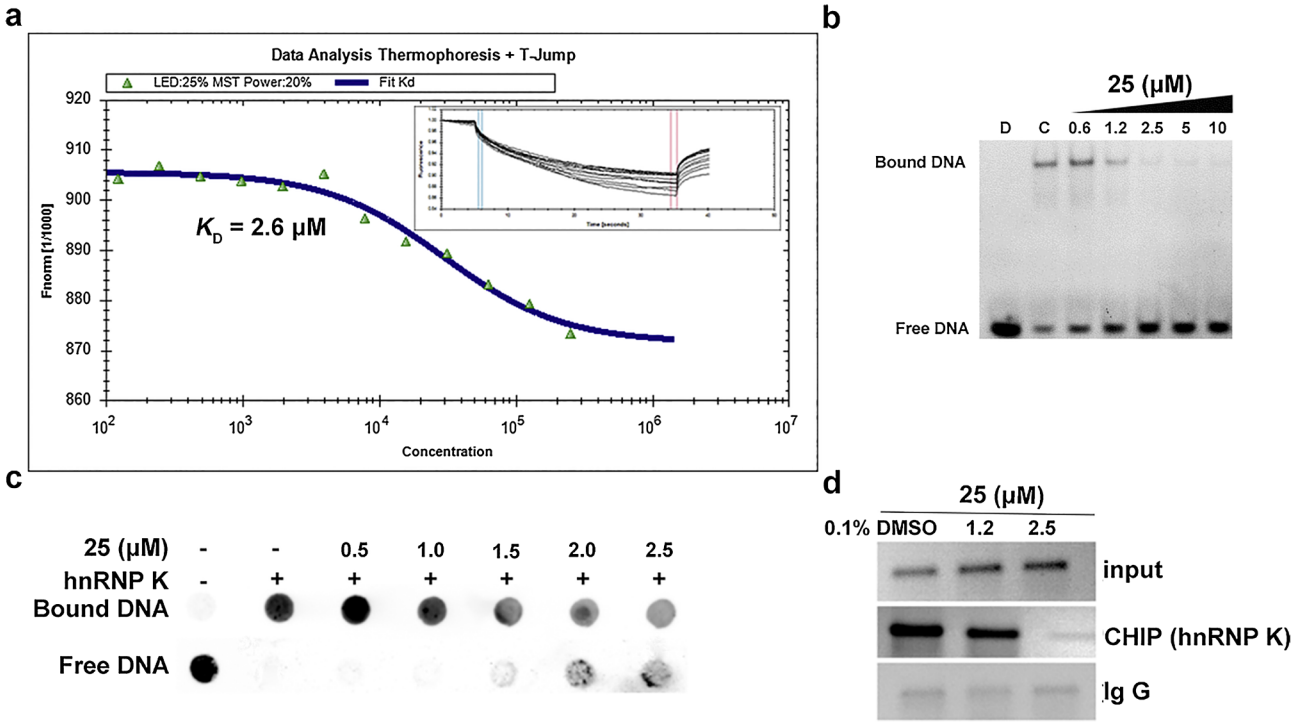

Fig. 3. The effect of compound **25** on the binding between hnRNP K and *c-myc* Py33. (a) Binding affinity of compound **25** to hnRNP K measured by using MST; (b) The effect of compound **25** on the binding between hnRNP K and *c-myc* Py33 measured through EMSA (D: Py33 only; C: hnRNP K plus Py33); (c) The effect of compound **25** on the binding between hnRNP K and *c-myc* Py33 measured through filter binding assay; (d) ChIP assay was carried out with antibody against hnRNP K in Hela cells. The cells were treated with DMSO (as a control) or compound **25**, respectively.

(**36–37**), however, all these derivatives had significantly reduced binding affinity, indicating that the unsaturated ketone is important for the binding affinity. The methylation derivative **35** also showed significantly reduced binding affinity, possibly because the methylation could affect the charge distribution of the Quinoline ring. Among our synthetic compounds, compound **25** exhibited the best binding affinity (4.6 μM, Table 1 and Fig. S5) and was much better than the hit compound **Q16** (20.1 μM).

In order to confirm the binding affinity of compound **25** to hnRNP K, microscale thermophoresis (MST) experiment was performed, since it is a sensitive method for quantitative analysis of molecular interactions [46]. As shown in Fig. 3**a**, our results showed that compound **25** could bind to hnRNP K with K_D value of 2.6 μM, which was consistent with our above SPR result. In order to know whether compound **25** could bind to i-motif DNA or duplex DNA, we also studied their binding interactions through MST. As shown in Fig. S6a and b, binding affinities of compound **25** to i-motif DNA and duplex DNA were found to be much weak, which could be ignored compared with its binding affinity to hnRNP K. These results indicated that compound **25** could selectively bind to hnRNP K without significant interaction with *c-myc* promoter DNA.

2.5. Quinoline derivatives inhibited various carcinoma cells proliferation

We employed MTT assay to evaluate the anti-proliferation activities of the Quinoline derivatives on various human cancer cell lines, such as human cervical cancer cell line Siha, human lung adenocarcinoma cell line A549, human squamous cervical cancer line Hela, human bone osteosarcoma epithelial cell line U2OS, human melanoma cell line A375, human hepatocellular carcinoma cell line HuH7. Human embryonic kidney cell line HEK293 was used as a normal cell control (low expression of hnRNP K). The cytotoxicity of the Quinoline derivatives was determined with their IC_{50} values as shown in Table 2. Most of the Quinoline derivatives **07–30** showed diverse cytotoxicity against various tumor cells. The derivatives with resonance electron donating R^1 substitutive groups, such as -OCH_3 (**7**, **13**, **19**, and **25**) and -OH (**11**, **17**, **23**, and **29**), showed generally strong cytotoxicity against most

Table 2
IC_{50} values for effect of Quinoline derivatives against different cell lines after 48 h incubation as determined by using MTT assay.

Comp.	IC_{50} (μM)						
	Siha	A549	Hela	U2OS	A375	HuH7	HEK293
7	3.28	0.79	2.38	3.81	2.60	1.63	44.71
8	3.75	3.15	1.69	2.04	9.31	2.02	40.07
9	0.72	0.74	1.17	3.53	3.48	0.32	15.32
10	> 50	> 50	> 50	> 50	> 50	> 50	47.86
11	4.05	4.34	2.13	3.94	1.88	1.97	12.58
12	7.75	7.19	12.07	1.47	8.44	1.51	21.15
13	0.79	0.28	2.88	1.40	1.05	1.14	13.03
14	3.05	0.22	3.48	2.78	4.74	5.43	29.17
15	2.88	0.89	3.11	1.83	2.71	1.14	11.73
16	3.08	2.71	3.25	1.62	2.49	6.23	34.60
17	3.80	3.77	5.14	0.79	1.99	2.54	12.05
18	2.67	2.07	6.89	2.45	0.77	1.43	13.48
19	4.07	3.37	2.86	1.88	6.58	1.29	12.92
20	2.38	0.30	4.24	3.17	2.73	4.75	45.18
21	3.45	0.29	3.77	1.33	1.96	1.05	11.83
22	9.41	2.51	7.25	2.10	7.90	6.21	35.12
23	15.49	18.05	4.02	1.43	5.12	1.91	21.64
24	13.31	5.98	15.87	1.52	0.49	1.60	16.53
25	3.52	3.04	2.21	1.36	3.59	2.94	34.72
26	28.18	19.48	11.98	4.50	8.92	9.41	23.11
27	3.28	13.42	13.19	1.34	5.58	9.58	18.30
28	10.76	13.28	21.45	2.25	6.91	10.76	12.41
29	2.12	1.19	2.01	1.51	4.02	2.68	17.07
30	12.62	29.63	28.25	2.35	5.39	4.04	21.01
31	> 50	> 50	> 50	> 50	> 50	> 50	> 50
32	> 50	> 50	> 50	18.91	> 50	> 50	> 50
33–36	> 50	> 50	> 50	> 50	> 50	> 50	> 50
37	> 50	> 50	> 50	22.42	> 50	> 50	> 50

types of cancer cells but weak cytotoxicity against HEK293, indicating that introduction of electron donating group into the R^1 position could increase the selectivity against tumor cells. In comparison, R substitutive groups seem to have less significant effect on the selectivity. The compounds **7**, **13**, **19**, and **25**, with R substitutive group of -OCH_3, -H, -F, and -NO_2, showed similar cytotoxicity against cancer cells. The hydroxylation derivatives (**31**–**33**), propylamine derivative (**34**), methylation derivative (**35**), and reduced derivatives (**36**–**37**), all showed very weak cytotoxicity against cancer cells, indicating that unsaturated ketone structure could be important for proliferation inhibition activity. Generally, the structure-activity relationship for the Quinoline derivatives against cancer cells was well consistent with that for inhibition of hnRNP K measured through SPR. Compound **25** is among the best of these compounds inhibited the proliferation of various carcinoma cell lines, with its IC_{50} values ranged from 1.36 to 3.59 μM. Our result showed that compound **25** had very low cytotoxicity against HEK293 normal cells (Table 2). These results indicated that compound **25** had potent and selective cytotoxicity against tumor cells possibly through inhibition of hnRNP K. As mentioned before, compound **25** had the best binding affinity (4.6 μM, Table 1) to hnRNP K, and therefore, was selected for further in-depth investigation.

2.6. The binding of compound *25* to hnRNP K disrupted the interaction between hnRNP K and c-myc gene promoter i-motif in vitro and in cells

As mentioned above, compound **25** appeared to be the most potent binding ligand to hnRNP K. In order to understand its effect on the binding interaction between hnRNP K and *c-myc* gene promoter i-motif, we performed several other experiments, including electrophoretic mobility shift assay (EMSA), filter binding assay, FRET assay, and Chromatin immunoprecipitation experiment (ChIP).

Firstly we used EMSA to study the effect of compound **25** on the binding interaction between hnRNP K and *c-myc* gene promoter. As shown in Fig. 3b, in the absence of compound **25** and hnRNP K, only free i-motif DNA appeared on the gel. Upon addition of hnRNP K, free DNA was depleted and the hnRNP K-DNA complex appeared on the gel. When increasing the concentration of compound **25**, the amount of the hnRNP K-DNA complex decreased, and free i-motif DNA increased, which indicated that the binding of compound **25** to hnRNP K could disrupt the binding interaction between hnRNP K and *c-myc* gene promoter i-motif. These results were also consistent with our filter binding assay data, as shown in Fig. 3c. Upon addition of increasing concentration of compound **25**, the amount of the hnRNP K-DNA complex gradually decreased, while the corresponding free i-motif DNA increased, indicating that the binding of compound **25** to hnRNP K could disrupt the binding interaction between hnRNP K and *c-myc* gene promoter i-motif in a dose-dependent manner.

As mentioned above, our hnRNP K could unfold *c-myc* promoter i-motif as studied by using CD and FRET assay. In the present investigation, FRET assay was used to study whether compound **25** could affect hnRNP K's unwinding function for *c-myc* promoter i-motif. As shown in Fig. S7, hnRNP K could unfold *c-myc* promoter i-motif, as indicated by decreased fluorescence intensity at 580 nm. After compound **25** was added, the unwinding activity of hnRNP K for i-motif was suppressed, as indicated by increased fluorescence intensity at 580 nm. These results suggested that the binding of compound **25** to hnRNP K could disrupt the interaction between hnRNP K and *c-myc* promoter i-motif.

Next, we performed ChIP experiment [45] in Hela cervical cancer cells to study whether compound **25** could inhibit the binding of hnRNP K to *c-myc* promoter DNA with a Magna ChIP™ Kit (Millipore) following the manufacturer's protocol. As shown in Fig. 3d, after incubation with 1.25 and 2.5 μM compound **25** for 24 h, we found that compound **25** could cause dose-dependent dissociation of hnRNP K from *c-myc* promoter DNA. Amplification of these immunoprecipitated samples showed a decrease of hnRNP K-bound DNA with increasing concentration of compound **25** in a dose dependent manner, indicating that compound **25** indeed disrupted the binding of hnRNP K with *c-myc* promoter DNA in Hela cells. All above results showed that the binding of compound **25** to hnRNP K could disrupt the interaction between hnRNP K and *c-myc* promoter DNA *in vitro* and in cells.

2.7. Molecular docking studies for the effect of compound *25* on the binding of hnRNP K with c-myc gene promoter NHE III_1

It has been known that the full length hnRNP K contains three KH domains (KH1, KH2 and KH3), which are closely related to the biological function of hnRNP K protein in recognizing RNA and DNA. KH3 domain has shown the strongest binding affinity to C-rich single-stranded DNA. Only crystal structure of the KH3 domain responsible for binding to C-rich single-stranded DNA is available for docking study. A molecular docking study was performed to investigate the binding mode and to help understand the bioactivity results. The mode was derived by docking and energy minimization of compound **25** in the ssDNA/RNA binding site of the KH3_hnRNP K (PDB ID: 1ZZI) [47]. The energy-minimized, top-ranked pose of compound **25** in the protein was displayed in Fig. S8a and b. Compound **25** was found to bind well with ssDNA-binding site, which interfered with the binding of hnRNP K to ssDNA. As shown in Fig. S8b, compound **25** was found to interact with residues Asp23, Ala25, Gly26, Ser27, Ile28, Lys31, Gly33, Gln34, Gln83, and Ser85 of KH3 hnRNP K protein, resulting in disrupting the binding of the protein to ssDNA. The ketone carbonyl group of compound **25** was found to have two hydrogen bonding interactions with Gln83 and Ser85 with distances of 3.3 Å and 3.1 Å, respectively. The methoxy group of compound **25** was found to bind to a narrow site of the protein as shown in Fig. S8a and b, which had a hydrogen bonding interaction with Gln34 with a distance of 3.0 Å. In contrast, the electron-withdrawing nitryl group on the other side of compound **25** had no strong binding interaction with the protein. These docking results are well consistent with our experimental results, which explained the importance of the ketone carbonyl group and methoxy substitutive group. It should be noted that the ketone carbonyl group is conjugated with the Quinoline ring and surrounded by several rings, which should make it electronically and sterically unfavorable to become Michael acceptor attacked by general nucleophiles. These docking results could be useful for further optimization of compound **25** and comparison with previous docking data of other compounds.

2.8. Compound *25* down-regulated c-myc gene transcription and translation

c-myc proto-oncogene encodes a multifunctional transcription factor that plays a critical role in a broad range of cellular processes, including the regulation of cell cycle progression, cell growth, differentiation, transformation, angiogenesis, and apoptosis [2,48,49]. Dysregulation of *c-myc* could arise through a variety of mechanisms, including chromosomal translocation [50], gene amplification [51], and increased transcription [1] as well as a higher rate of translation and enhanced protein stability [17]. Since hnRNP K has been shown to be a positive-acting transcription factor for human *c-myc* gene, we further studied whether the effect of compound **25** on hnRNP K could influence *c-myc* gene transcription. Considering hnRNP K showed higher level of expression in Hela cells [52], we chose Hela cells to study the effect of compound **25** on c-*myc* gene transcription and expression through RT-PCR and Western blot. After incubation with varying concentration of compound **25** for 3 h, the total RNA was extracted with a RNA extraction kit and reversely transcripted to cDNA. The cDNA was then used as a template for quantitative PCR amplification of the *c-myc* gene, with β-actin as a control. As shown in Fig. 4a and b, the incubation with increasing concentration of compound **25** caused a reduction of *c-myc* mRNA in a dose-dependent manner in Hela cells. Western blot was also carried out to measure c-MYC protein expression levels, as shown in

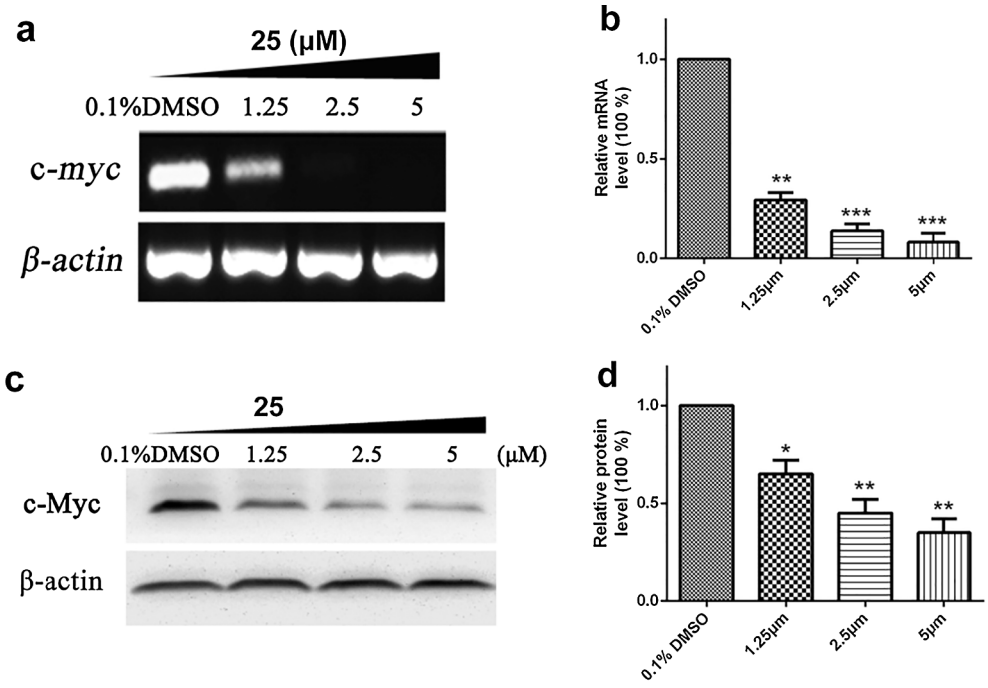

Fig. 4. Compound **25** down-regulated transcription and expression of *c-myc* gene. (a) RT-PCR experiment for Hela cells treated with 0.1% DMSO and compound **25** ranged from 0 to 5 μM for 48 h; (b) Optical density analysis for the result of RT-PCR on *c-myc* gene transcription; (c) Western blot for Hela cells treated with 0.1% DMSO and compound **25** ranged from 0 to 5 μM for 48 h. (d) Optical density analysis for c-MYC protein expression. The symbol * indicates a significant difference at $P < 0.05$; the symbol ** indicates a significant difference at $P < 0.01$; the symbol *** indicates a significant difference at $P < 0.001$.

Fig. 4c and d. Upon incubation with increasing concentration of compound **25**, the expression levels of c-MYC also decreased in a dose-dependent manner. These results indicated that compound **25** could down-regulate *c-myc* gene transcription and expression in Hela cells in a dose-dependent manner possibly through its inhibition of hnRNP K.

2.9. Effect of compound 25 on Hela cells apoptosis and apoptosis-related protein expressions

It has been previously reported that a decreasing expression of c-MYC may induce cellular apoptosis of proliferating cancer cells. As our above studies showed that compound **25** could bind to hnRNP K and down-regulate *c-myc* transcription and expression, we analyzed Hela cells apoptosis upon incubation with compound **25**. As shown in Fig. 5a and b, upon incubation of Hela cells with compound **25** at increasing concentration of 0, 1.25, 2.5, and 5.0 μM for 24 h, both early and late cell apoptosis were induced. The percentages of early apoptosis cells were 1.06% 12.72%, 29.30%, and 48.49%, while the percentages of late apoptosis cells were 0.33%, 2.74%, 5.59%, and 6.29%, respectively. Besides, we also investigated the expression of proteins in the cell apoptosis regulation pathway through Western blot after incubation with increasing concentration of compound **25**. As shown in Fig. 5c, dose-dependent increases in apoptosis related proteins, such as cleaved caspase-3 and cleaved PARP, were observed. Compound **25** down-regulated the expression of caspase-3 and PARP, which were related to cellular apoptosis process. Our above results of Hela cells apoptosis induced by compound **25** could be due to its repression of *c-myc* transcription, which are well consistent with previously reported results.

2.10. Compound 25 could inhibit tumor cells proliferation, migration and invasion

hnRNP K has been shown to be closely involved in metastasis and related with gallbladder carcinoma, prostate cancer, and colorectal cancer metastasis [52,53]. hnRNP K regulates metastasis *in vivo* by regulation of extra-cellular matrix components through the ERK signaling pathway [17]. As mentioned above, compound **25** could have significant inhibitory effect on the proliferation of Hela cells in short-term proliferation with an IC_{50} value of 2.21 μM. The inhibitory effect of compound **25** on cell proliferation was further investigated through colony formation assay, scrape assay, and transwell assay, in order to study its inhibition of tumor cells long-term proliferation, metastasis, and invasion, respectively. As shown in Fig. S9a, upon incubation with compound **25**, colony formation obviously decreased, suggesting inhibition of cell proliferation, which was consistent with our MTT results. In comparison, compound **25** had no significant effect on HEK293 cells (normal cells), as shown in Fig. S9b. Our results in scrape assay indicated that compound **25** could inhibit metastasis in a dose-dependent manner as shown in Fig. 6a. Next, the Hela cells were incubated with 1.25 μM compound **25** for 24 h, and the cells migration was reduced for approximately 68% as shown in Fig. 6b. This result was in good agreement with that of the cell scratch assay, indicating that compound **25** could inhibit Hela cells invasion. The above results suggested that compound **25** could inhibit proliferation, metastasis, and invasion of cancer cells, which could be due to its repression of *c-myc* transcription.

2.11. Compound 25 inhibited tumor growth in a Hela cervical xenograft

To further demonstrate that compound **25** as a hnRNP K inhibitor could be useful for cancer treatment, we tested compound **25** in a Hela xenograft mouse model of human cervical cancer. When the tumor size reached approximately 100 mm^3, the mice were randomly divided into four groups (seven mice per group) for intraperitoneal injection (ip) daily including: the vehicle group, compound **25** 6.7 mg/kg treated group, compound **25** 20.0 mg/kg treated group, and Cisplatin 1.0 mg/kg treated group [29,30]. The tumors were collected after 3 weeks of treatment and analyzed. As shown in Fig. 7a–b and Fig. S10a–b, compared with the vehicle group (mean of 1000.1 mg), the treatment with compound **25** at 6.7 mg/kg and 20.0 mg/kg resulted in a statistically significant reduction in tumor weight with a tumor growth inhibition rate (**IR**) of 54.1% and 69.3%, respectively (mean values of 459.7 mg and 307.4 mg, respectively). The wide-spectrum antitumor drug Cisplatin was used as a positive control (**IR** = 83.2%, mean, 168.2 mg). Meanwhile, the results of tumor weight from each group were consistent with results of tumor volume. The treatment with compound **25** at 6.7 mg/kg and 20.0 mg/kg resulted in a significant decrease in the

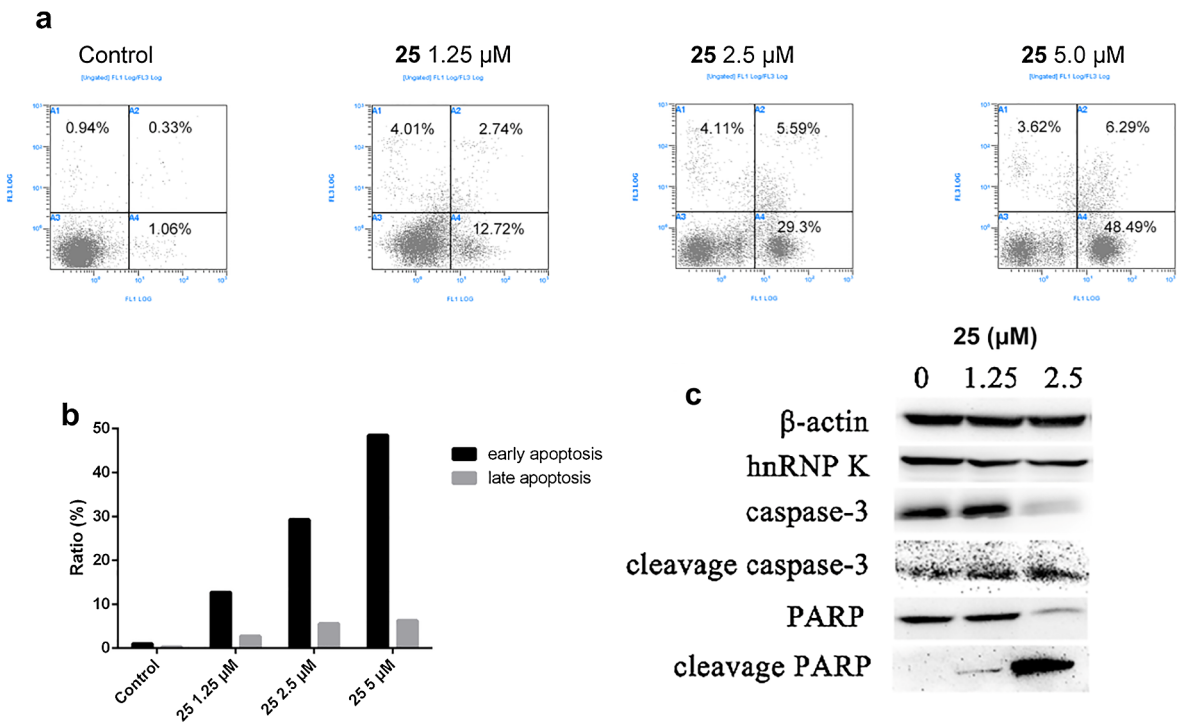

Fig. 5. Effect of compound **25** on Hela cells apoptosis and apoptosis-related protein expressions. (a) Hela cells were incubated with increasing concentration of compound **25** for 24 h, and then stained with annexin-V and propidium iodide (PI) before analysis for apoptotic cell death. Viable cells are presented as both annexin-V and PI negative. (b) The data were analyzed for early apoptosis and later apoptosis. (c) The total protein was harvested for Western blot analysis of the expression levels of the apoptosis-related proteins including caspase-3, cleaved caspase-3, PARP, and cleaved-PARP.

final tumor volume (means of 474.1 mm^3 and 326.3 mm^3, respectively) compared to the vehicle group (mean of 1114.9 mm^3, Fig. 7a). Our data showed that the inhibition of tumor growth after treatment with compound **25** was in a time-dependent manner. As shown in Fig. 7c, no significant differences in body weights were observed among the vehicle group, compound **25** treated groups, and Cisplatin treated group. Compound **25** neither altered cellular morphology nor induced pathological changes in the heart, liver, spleen, and kidney (Figs. 7d and S10c), indicating that it was tolerated well at these doses. These data showed that compound **25** exhibited a good antitumor activity for the inhibition of Hela cervical cancer growth in BALB/C-nu/nu mice with Hela xenografts through the suppression of proliferation *in vivo*.

3. Conclusion

In this study, we synthesized a series of new Quinoline derivatives and evaluated their binding affinity for hnRNP K. Among these derivatives, we found that compound **25** could bind to hnRNP K with the K_D value determined to be 4.6 and 2.6 μM by using SPR and MST, respectively. The binding of compound **25** to hnRNP K could disrupt its interaction with *c-myc* promoter i-motif and down-regulate c-*myc* gene expression. Compound **25** could inbit the proliferation of various human cancer cell lines with IC_{50} values ranged from 1.36 to 3.59 μM. Compound **25** could induce Hela cells apoptosis, and inhibit tumor cells long-term proliferation, migration and invasion. Compound **25** exhibited good tumor growth inhibition in a Hela xenograft tumor model with a statistically significant reduction of tumor weight, which might be related to its ability of binding to hnRNP K. As the first binding ligand for protein of hnRNPs family, compound **25** might be further modified for discovery of new binding ligands for other proteins of hnRNPs family. It should be noted that DNA secondary structures including G-quadruplexes and i-motifs have been widely characterized and believed to play key roles as transcriptional repressors, and a variety of ligands binding to and stabilizing G-quadruplexes and i-motifs have caused the suppression of gene transcription and expression. However, due to wide abundance of these types of DNA secondary structures in genomic sequence, the selective targeting by small molecule ligands is a potential problem. The overexpression of hnRNP K is associated with development of various cancers, and tumor cells rely on hnRNP K to turn on or up-regulate certain gene transcriptions partly

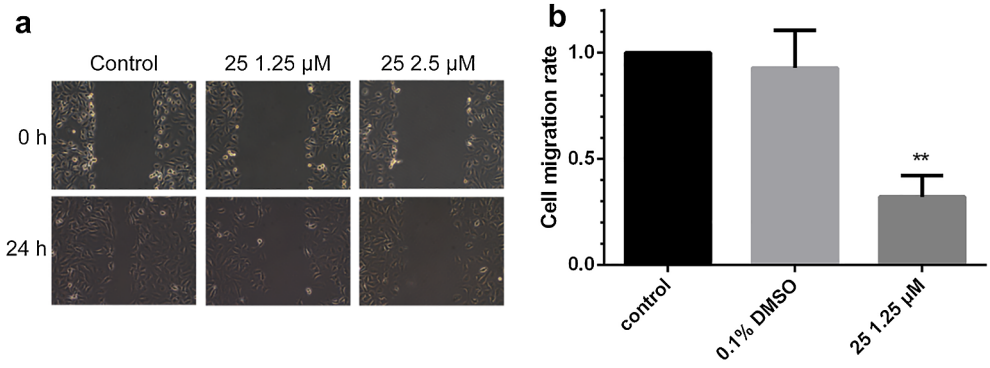

Fig. 6. Effect of compound **25** on Hela cells migration and invasion. (a) Compound **25** suppressed the migration of Hela cells in a dose-dependent manner in cell scrape experiment. A cross-shaped scrape was made after the cells were confluent as a monolayer, and then the cells were incubated with different concentrations of compound **25** for 0 and 24 h. (b) Quantification of Hela cells invasion in transwell assays in the absence or presence of compound **25**. All experiments were repeated for three times, and the symbol ** indicates a significant difference at $P < 0.01$.

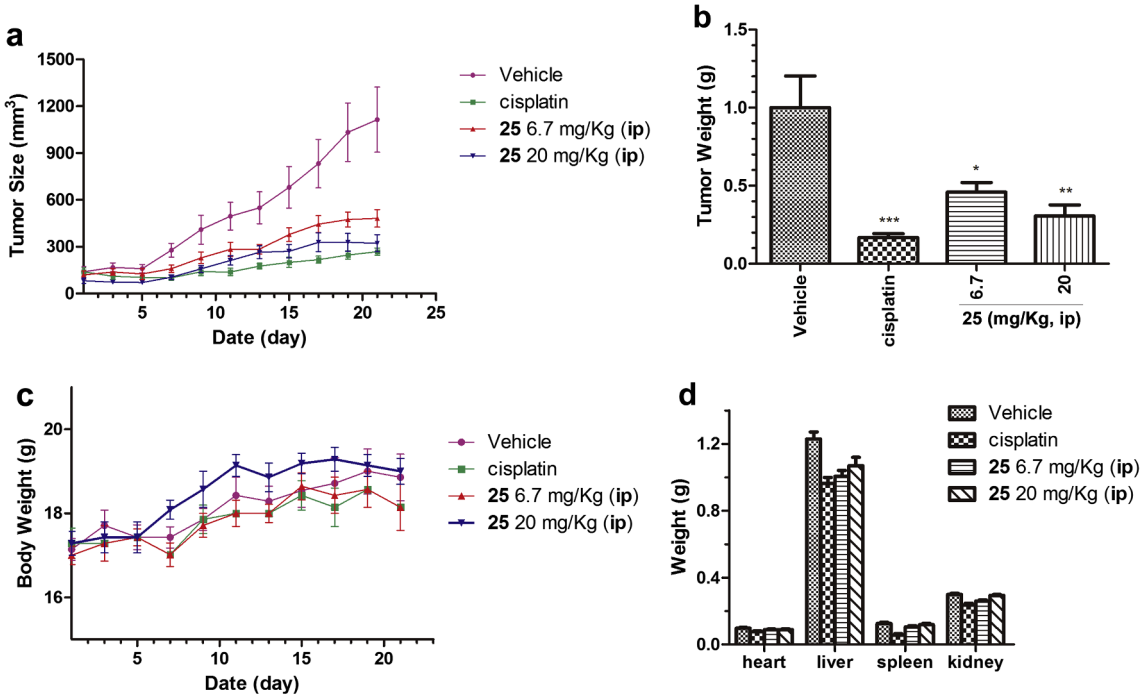

Fig. 7. Compound **25** inhibited tumor growth in a Hela xenograft model. Compound **25**, Cisplatin, and saline (as vehicle) were administered through ip injection to athymic nude mice with human tumor xenografts established using Hela cells. The mice were injected ip once a day for three weeks. Vehicle controls were injected with 100 μL of saline. The positive control group received Cisplatin through ip injection at a dose of 1 mg/kg, once a day. Compound **25** was similarly administered to mice, once a day, at doses of 6.25 and 20 mg/kg, respectively. (a) The tumor sizes were measured and recorded every two days. The tumor volumes were calculated from sizes measured and recorded every day. The volume (mm^3) = length (mm) × width $(mm)^2/2$. (b) The tumor weight at the end of treatment. The inhibition rate (IR) was calculated using (tumor weight in drug-treatment group)/(tumor weight in vehicle group) and indicated on the column. Two-tailed unpaired student's t tests were applied for tumor weight statistical analysis: the symbol * and ** indicates a significant difference at $P < 0.05$ and $P < 0.01$, respectively, compared to vehicle. (c) The body weights were measured and recorded every two days. (d) Organs weights of the mice in each group at the end of the observation period.

through its binding with promoter C-rich sequences/i-motifs. hnRNP K could have different binding affinity and selectivity to various C-rich sequences/i-motifs in transcriptional regulation, therefore, our present study for inhibition of hnRNP K by small molecule ligands could offer a potentially new and more selective strategy of regulating oncogene transcription by taking advantage of the selectivity of hnRNP K for different C-rich sequences/i-motifs in gene promoter.

4. Materials and methods

4.1. General method for synthesis

All chemicals were purchased from commercial sources, which were analytical grade without further purification unless otherwise specified. All synthesized compounds were confirmed by using ^1H, ^{13}C NMR spectra and HRMS spectrometry. ^1H and ^{13}C NMR spectra were recorded using TMS as the internal standard in DMSO-d_6, CD_3OD, or $CDCl_3$ with a Bruker BioSpin GmbH spectrometer at 400 and 100 MHz, respectively. High resolution mass spectra (HRMS) were recorded on Shimadzu LCMS-IT-TOF of MAT95XP mass spectrometer (Thermo Fisher Scientific, USA). The purity of the synthesized compounds was confirmed to be higher than 95% by using analytical HPLC performed with a dual pump Shimadzu LC-20 AB system equipped with an Ultimate XB-C18 column (4.6 mm × 250 mm, 5 μm), eluting with methanol-water (10:90 to 60:40) containing 0.05% TFA at a flow rate of 0.5 mL/min. The synthetic pathway for Quinoline derivatives **07–37** was shown in Scheme 1.

4.1.1. General procedure for the preparation of 2-methyl-6-substituted-quinolin-4-ol (2a–d)

To a solution of 4-substituted aniline (**1a–d**, 72.4 mmol) in PPA (150 g), was added ethyl acetoacetate (18.8 g, 14.5 mmol) dropwise. The reaction mixture was stirred at 120 °C until the **1a–d** was consumed monitored with TLC. After cooling down to 70 °C, the mixture was poured into ice water and stirred, with pH adjusted to 9–10 by adding ammonium hydroxide. Then the mixture was filtered, and the solid was washed with water for three times and dried under reduced pressure to give the crude **2a–d**, which was used directly for the next step reaction without any purification.

4.1.2. General procedure for the preparation of 4-chloro-2-methyl-6-substituted-quinoline (3a–d)

To a solution of **2a–d** (4.0 g, crude) in dioxane (60 mL), was added $POCl_3$ (10 mL) dropwise at 0–5 °C, followed with DMF (0.3 mL). The mixture was then heated to 100 °C, and reacted for 4 h. After cooling down to room temperature, the solvent was removed, and the residue was poured into ice water with stirring. After addition of ethyl acetate (50 mL), pH was adjusted to 9–10 by adding sodium bicarbonate, the mixture was filtered and the organic phase was extracted with ethyl acetate (20 mL × 3). The combined organic layer was washed with brine, dried over anhydrous sodium sulfate, filtered, and then concentrated under reduced pressure. The residue was purified by using silica gel chromatograph with petroleum ether/ethyl acetate (10/1–3/1) to give the desire compound **3a–d** with yield of 45–57% for two steps.

4.1.2.1. 4-chloro-6-methoxy-2-methylquinoline (3a). The compound was obtained as a yellow solid with a yield of 57%. ^1H NMR (400 MHz, $CDCl_3$) δ 7.79 (d, J = 5.0 Hz, 1H), 7.57 (d, J = 3.1 Hz, 1H), 7.34 (dd, J = 11.0, 2.9 Hz, 1H), 7.13 (s, 1H), 3.81 (s, 3H), 2.68 (s, 3H). ESI-MS (m/z) 208 $[M+H]^+$.

4.1.2.2. 4-chloro-2-methylquinoline (3b). The compound was obtained as a light yellow solid with a yield of 51%. ^1H NMR (400 MHz, $CDCl_3$) δ

8.13 (dd, J = 7.5, 1.6 Hz, 1H), 8.05 (dd, J = 7.4, 1.5 Hz, 1H), 7.71–7.62 (m, 1H), 7.62–7.55 (m, 1H), 7.22 (s, 1H), 2.68 (s, 3H). ESI-MS (m/z) 178 $[M+H]^+$.

*4.1.2.3. 4-chloro-6-fluoro-2-methylquinoline (**3c**)*. The compound was obtained as a light yellow solid with a yield of 54%. ^{1}H NMR (500 MHz, $CDCl_3$) δ 8.04 (dd, J = 7.5, 5.0 Hz, 1H), 7.74 (dd, J = 7.9, 1.4 Hz, 1H), 7.46–7.33 (m, 1H), 7.20 (s, 1H), 2.68 (s, 3H). ESI-MS (m/z) 196 $[M+H]^+$.

*4.1.2.4. 4-chloro-2-methyl-6-nitroquinoline (**3d**)*. The compound was obtained as a yellow solid with a yield of 45%. ^{1}H NMR (400 MHz, $CDCl_3$) δ 9.11 (t, J = 3.1 Hz, 1H), 8.49 (dt, J = 9.2, 2.5 Hz, 1H), 8.14 (t, J = 4.6 Hz, 1H), 7.55 (s, 1H), 2.79 (s, 3H). ESI-MS (m/z) 223 $[M+H]^+$.

*4.1.3. General procedure for the preparation of 4-(2-methyl-6-substituted-quinolin-4-yl)morpholine (**4a–d**)*

To a solution of **3a–d** (2.25 mmol) in morpholine (2 mL), was added 4-methylbenzenesulfonic acid (Ts-OH, 50.0 mg). The reaction mixture was stirred at 120 °C for 3 h until the TLC showed complete reaction. After cooling down, the mixture was powered into ice water and stirred. The organic layer was extracted with ethyl acetate (3 × 10 mL). The combined organic layer was washed with brine for three times, dried over anhydrous sodium sulfate, filtered, concentrated and the residue was purified by using silica gel chromatograph with petroleum ether/ethyl acetate (4/1–1/1) to give compound **4a–d** with yield of 75–82%.

*4.1.3.1. 4-(6-methoxy-2-methylquinolin-4-yl)morpholine (**4a**)*. The compound was obtained as a light yellow solid with a yield of 80%. ^{1}H NMR (400 MHz, $CDCl_3$) δ 7.92 (d, J = 8.9 Hz, 1H), 7.30 (d, J = 9.2 Hz, 1H), 7.27 (s, 1H), 6.75 (s, 1H), 4.03–3.96 (m, 4H), 3.92 (s, 3H), 3.23–3.15 (m, 4H), 2.67 (s, 3H). ESI-MS (m/z) 259 $[M+H]^+$.

*4.1.3.2. 4-(2-methylquinolin-4-yl)morpholine (**4b**)*. The compound was obtained as a yellow solid with a yield of 80%. ^{1}H NMR (400 MHz, $CDCl_3$) δ 8.27 (d, J = 8.3 Hz, 1H), 7.98 (d, J = 8.3, 1H), 7.68–7.36 (m, 2H), 7.08 (s, 1H), 3.71 (t, J = 9.2 Hz, 4H), 3.17 (t, J = 9.3 Hz, 4H), 2.52 (s, 3H). ESI-MS (m/z) 229 $[M+H]^+$.

*4.1.3.3. 4-(6-fluoro-2-methylquinolin-4-yl)morpholine (**4c**)*. The compound was obtained as a light yellow solid with a yield of 82%. ^{1}H NMR (400 MHz, $CDCl_3$) δ 7.99 (dd, J = 11.9, 5.0 Hz, 1H), 7.61 (dd, J = 11.0, 5.3 Hz, 1H), 7.52–7.26 (m, 1H), 7.10 (s, 1H), 3.72 (t, J = 8.4 Hz, 4H), 3.18 (t, J = 8.4 Hz, 4H), 2.53 (s, 3H). ESI-MS (m/z) 247 $[M+H]^+$.

*4.1.3.4. 4-(2-methyl-6-nitroquinolin-4-yl)morpholine (**4d**)*. The compound was obtained as a yellow solid with a yield of 75%. ^{1}H NMR (400 MHz, $CDCl_3$) δ 8.91 (d, J = 2.6 Hz, 1H), 8.38 (dt, J = 5.7, 2.8 Hz, 1H), 8.05 (dd, J = 9.2, 5.0 Hz, 1H), 6.86 (s, 1H), 4.04 (t, J = 9.2 Hz, 4H), 3.27 (t, J = 8.8 Hz, 4H), 2.73 (s, 3H). ESI-MS (m/z) 274 $[M+H]^+$.

*4.1.4. General procedure for the preparation of 4-morpholino-6-substituted-quinoline-2-carbaldehyde (**5a–d**)*

To a solution of **4a–d** (1.47 mmol) in dioxane (10 mL), was added selenium dioxide (244 mg, 2.20 mmol). The reaction mixture was stirred at 100 °C for 3 h. After cooling down to room temperature, the mixture was filtered, concentrated and the residue was purified by using silica gel chromatograph with petroleum ether/ethyl acetate (6/1–2/1) to give compound **5a–d** with yield of 61–78%.

*4.1.4.1. 6-methoxy-4-morpholinoquinoline-2-carbaldehyde (**5a**)*. The compound was obtained as a light yellow solid with a yield of 78%. ^{1}H NMR (400 MHz, $CDCl_3$) δ 10.12 (s, 1H), 8.12 (d, J = 9.2 Hz, 1H), 7.51 (s, 1H), 7.43 (dd, J = 9.2, 2.8 Hz, 1H), 7.33 (d, J = 2.8 Hz, 1H), 4.00 (d, J = 4.6 Hz, 4H), 3.98 (s, 3H), 3.26 (d, J = 4.6 Hz, 4H). ESI-MS (m/z) 273 $[M+H]^+$.

*4.1.4.2. 4-morpholinoquinoline-2-carbaldehyde (**5b**)*. The compound was obtained as a light yellow solid with a yield of 70%. ^{1}H NMR (400 MHz, $CDCl_3$) δ 10.16 (s, 1H), 8.21 (d, J = 8.4 Hz, 1H), 8.07 (d, J = 8.4 Hz, 1H), 7.80–7.73 (m, 1H), 7.66–7.60 (m, 1H), 7.49 (s, 1H), 4.01 (d, J = 4.6 Hz, 4H), 3.30 (d, J = 4.6 Hz, 4H). ESI-MS (m/z) 243 $[M+H]^+$.

*4.1.4.3. 6-fluoro-4-morpholinoquinoline-2-carbaldehyde (**5c**)*. The compound was obtained as a yellow solid with a yield of 69%. ^{1}H NMR (400 MHz, $CDCl_3$) δ 10.09 (s, 1H), 8.25 (d, J = 8.4 Hz, 1H), 7.89 (d, J = 9.2 Hz, 1H), 7.80–7.73 (m, 1H), 7.62–7.44 (m, 1H), 7.30 (s, 1H), 4.01 (t, J = 5.8 Hz, 4H), 3.30 (t, J = 5.8 Hz, 4H). ESI-MS (m/z) 261 $[M+H]^+$.

*4.1.4.4. 4-morpholino-6-nitroquinoline-2-carbaldehyde (**5d**)*. The compound was obtained as a yellow solid with a yield of 61%. ^{1}H NMR (400 MHz, $CDCl_3$) δ 10.19 (s, 1H), 9.00 (d, J = 2.5 Hz, 1H), 8.53 (dd, J = 9.2, 2.5 Hz, 1H), 8.43–8.27 (m, 1H), 7.57 (s, 1H), 4.07 (t, J = 5.6 Hz, 4H), 3.41 (t, J = 5.4 Hz, 4H). ESI-MS (m/z) 288 $[M+H]^+$.

*4.1.5. General procedure for the preparation of (E)-1-(4-substituted-phenyl)-3-(4-morpholino-6-substituted-quinolin-2-yl)prop-2-en-1-ones (**7–11, 13–17, 19–23,** and **25–29**)*

To a solution of 1-(4-substituted-phenyl)ethanone (**6a–e**, 1.84 mmol, 1.2 equiv) in 10 mL AcOH, was added aldehyde (**5a–d**, 1.54 mmol) with stirring slowly. After cooling down to 5 °C, concentrated H_2SO_4 (0.3 mL) was added slowly and carefully. The mixture was heated to 90 °C and reacted overnight. After cooling down to room temperature, the mixture was poured into ice water with stirring, and pH was adjusted to 9–10 by adding sodium carbonate. The solution was filtered, and the solid was washed with saturated sodium bicarbonate, dried and purified by using silica gel chromatograph with dichloromethane/MeOH (100/1–30/1) to give desire Quinoline derivative (**7–11**, **13–17**, **19–23** and **25–29**).

*4.1.6. General procedure for the preparation of (E)-1-(4-(benzyloxy) phenyl)-3-(4-morpholino-6-substituted-quinolin-2-yl)prop-2-en-1-ones (**12, 18, 24** and **30**)*

To a solution of 1-(4-(benzyloxy)phenyl)ethanone (**6f**, 416 mg, 1.84 mmol, 1.2 equiv) in 10 mL EtOH, was added aldehyde (**5a–d**, 1.54 mmol) at 5 °C. The reaction mixture was stirred until TLC indicated complete reaction. The solution was filtered under reduced pressure, and the solid was washed with cold EtOH (3 × 2 mL), dried and recrystallized in EtOH to give desired compound (**12**, **18**, **24**, and **30**).

*4.1.6.1. (E)-3-(6-methoxy-4-morpholinoquinolin-2-yl)-1-(4-methoxyphenyl)prop-2-en-1-one (**7**)*. Compound **5a** was reacted with 1-(4-methoxyphenyl)ethanone (**6a**) according to general procedure to afford compound **7** as a yellow solid with a yield of 75%. ^{1}H NMR (400 MHz, DMSO) δ 8.23 (d, J = 15.6 Hz, 1H), 8.18 (d, J = 8.8 Hz, 2H), 7.96 (d, J = 9.2 Hz, 1H), 7.76 (d, J = 15.6 Hz, 1H), 7.61 (s, 1H), 7.41 (dd, J = 9.2, 2.7 Hz, 1H), 7.28 (d, J = 2.7 Hz, 1H), 7.13 (d, J = 8.8 Hz, 2H), 3.97–3.92 (m, 7H), 3.89 (s, 3H), 3.24 (t, J = 4.0 Hz, 4H). ^{13}C NMR (101 MHz, DMSO) δ 188.08, 163.88, 157.85, 156.20, 152.20, 145.29, 144.15, 132.18, 131.52, 130.72, 125.91, 124.28, 122.17, 114.61, 109.69, 102.55, 66.68, 56.07, 55.87, 52.46. Purity was determined to be 99.7% by using HPLC. HRMS (ESI; m/z) calcd for C24H24N2O4, $[M+H]^+$, 405.1764; found 405.1831.

*4.1.6.2. (E)-3-(6-methoxy-4-morpholinoquinolin-2-yl)-1-phenylprop-2-en-1-one (**8**)*. Compound **5a** was reacted with acetophenone (**6b**) according to general procedure to afford compound **8** as a pale yellow solid with a yield of 61%. ^{1}H NMR (400 MHz, $CDCl_3$) δ 8.11 (d, J = 7.4 Hz, 2H), 8.04 (d, J = 9.8 Hz, 1H), 7.87 (d, J = 15.5 Hz, 1H), 7.61 (t, J = 7.3 Hz, 1H), 7.54 (d, J = 7.7 Hz, 2H), 7.51 (s, 1H), 7.38 (dd, J = 9.2, 2.8 Hz, 1H), 7.29 (d, J = 2.8 Hz, 1H), 7.13 (s, 1H), 4.02 (d,

J = 4.6 Hz, 4H), 3.96 (s, 1H), 3.26 (d, J = 4.6 Hz, 4H). ^{13}C NMR (101 MHz, $CDCl_3$) δ 190.87, 157.98, 151.53, 144.43, 137.96, 132.98, 132.17, 128.82, 128.67, 126.07, 126.00, 124.39, 121.94, 110.07, 101.96, 99.87, 66.95, 55.53, 52.34. Purity was determined to be 99.4% by using HPLC. HRMS (ESI; *m/z*) calcd for C23H22N2O3, $[M+H]^+$, 375.1658; found 375.1715.

*4.1.6.3. (E)-1-(4-fluorophenyl)-3-(6-methoxy-4-morpholinoquinolin-2-yl) prop-2-en-1-one (**9**).* Compound **5a** was reacted with 1-(4-fluorophenyl) ethanone (**6c**) according to general procedure to afford compound **9** as a yellow solid with a yield of 51%. ^{1}H NMR (400 MHz, DMSO) δ 8.32–8.16 (m, 3H), 7.96 (d, J = 9.2 Hz, 1H), 7.78 (d, J = 15.6 Hz, 1H), 7.63 (s, 1H), 7.50–7.36 (m, 3H), 7.29 (d, J = 2.7 Hz, 1H), 3.99–3.87 (m, 7H), 3.24 (t, J = 4.0 Hz, 4H). ^{13}C NMR (101 MHz, DMSO) δ 188.57, 166.89, 164.38, 157.95, 156.22, 151.98, 145.22 (d, J = 18.0 Hz), 134.51, 132.16 (t, J = 7.2 Hz), 125.72, 124.36, 122.23, 116.51, 116.29, 109.75, 102.57, 66.67, 55.89, 52.47. Purity was determined to be 99.6% by using HPLC. HRMS (ESI; *m/z*) calcd for C23H21FN2O3, $[M+H]^+$, 393.1609; found 393.1622.

*4.1.6.4. (E)-3-(6-methoxy-4-morpholinoquinolin-2-yl)-1-(4-nitrophenyl) prop-2-en-1-one (**10**).* Compound **5a** was reacted with 1-(4-nitrophenyl) ethanone (**6d**) according to general procedure to afford compound **10** as a yellow solid with a yield of 46%. ^{1}H NMR (400 MHz, $CDCl_3$) δ 8.45–8.35 (m, 2H), 8.30–8.21 (m, 2H), 8.15–8.02 (m, 2H), 7.92 (d, J = 15.4 Hz, 1H), 7.41 (dd, J = 9.2, 2.8 Hz, 1H), 7.32 (d, J = 2.7 Hz, 1H), 7.14 (s, 1H), 4.04 (d, J = 4.6 Hz, 4H), 3.99 (s, 3H), 3.28 (d, J = 4.6 Hz, 4H). ^{13}C NMR (101 MHz, $CDCl_3$) δ 189.34, 158.22, 156.20, 150.83, 150.18, 146.08, 145.71, 142.75, 132.23, 129.69, 124.97, 124.71, 123.90, 122.20, 110.49, 101.92, 66.93, 55.55, 52.33. Purity was determined to be 98.2% by using HPLC. HRMS (ESI; *m/z*) calcd for C23H21N3O5, $[M+H]^+$, 420.1553; found 420.1566.

*4.1.6.5. (E)-1-(4-hydroxyphenyl)-3-(6-methoxy-4-morpholinoquinolin-2-yl)prop-2-en-1-one (**11**).* Compound **5a** was reacted with 1-(4-hydroxyphenyl)ethanone (**6e**) according to general procedure to afford compound **11** as a yellow solid with a yield of 56%. ^{1}H NMR (400 MHz, DMSO) δ 10.49 (s, 1H), 8.21 (d, J = 15.6 Hz, 1H), 8.10 (d, J = 8.6 Hz, 2H), 7.95 (d, J = 9.2 Hz, 1H), 7.73 (d, J = 15.6 Hz, 1H), 7.61 (s, 1H), 7.41 (dd, J = 9.2, 2.4 Hz, 1H), 7.29 (d, J = 2.3 Hz, 1H), 6.94 (d, J = 8.6 Hz, 2H), 3.99–3.89 (m, 7H), 3.24 (t, J = 3.6 Hz, 4H). ^{13}C NMR (101 MHz, $CDCl_3$) δ 189.30, 162.33, 157.87, 156.34, 151.71, 144.98, 142.60, 131.37, 130.92, 129.37, 126.22, 124.30, 122.05, 115.40, 109.58, 101.94, 66.74, 55.29, 52.07. Purity was determined to be 95.3% by using HPLC. HRMS (ESI; *m/z*) calcd for C23H22N2O4, $[M+H]^+$, 391.1652; found 391.1662.

*4.1.6.6. (E)-1-(4-(benzyloxy)phenyl)-3-(6-methoxy-4-morpholinoquinolin-2-yl)prop-2-en-1-one (**12**).* Compound **5a** was reacted with 1-(4-(benzyloxy)phenyl)ethanone (**6f**) according to general procedure to afford compound **12** as a pale yellow solid with a yield of 64%. ^{1}H NMR (400 MHz, $CDCl_3$) δ 8.14 (d, J = 8.8 Hz, 2H), 8.12–8.01 (m, 2H), 7.86 (d, J = 15.4 Hz, 1H), 7.56–7.34 (m, 6H), 7.30 (d, J = 2.8 Hz, 1H), 7.16–7.05 (m, 3H), 5.17 (s, 2H), 4.02 (d, J = 4.6 Hz, 4H), 3.96 (s, 3H), 3.26 (d, J = 4.6 Hz, 4H). ^{13}C NMR (101 MHz, $CDCl_3$) δ 188.91, 162.74, 157.88, 156.03, 151.81, 145.69, 143.47, 140.79, 136.23, 132.15, 131.16, 128.71, 128.25, 127.51, 125.80, 124.44, 121.82, 114.74, 110.17, 101.95, 70.20, 66.96, 55.50, 52.34. Purity was determined to be 99.0% by using HPLC. HRMS (ESI; *m/z*) calcd for C30H28N2O4, $[M+H]^+$, 481.2121; found 481.2135.

*4.1.6.7. (E)-1-(4-methoxyphenyl)-3-(4-morpholinoquinolin-2-yl)prop-2-en-1-one (**13**).* Compound **5b** was reacted with **6a** according to general procedure to afford compound **13** as a yellow solid with a yield of 43%. ^{1}H NMR (400 MHz, DMSO) δ 8.29 (d, J = 15.6 Hz, 1H), 8.19 (d, J = 8.8 Hz, 2H), 8.07 (d, J = 8.3 Hz, 1H), 8.03 (d, J = 8.4 Hz, 1H), 7.81–7.72 (m, 2H), 7.61 (s, 1H), 7.58 (d, J = 7.3 Hz, 1H), 7.14 (d, J = 8.8 Hz, 2H), 3.92 (t, J = 7.3 Hz, 4H), 3.89 (s, 3H), 3.27 (t, J = 7.3 Hz, 4H). ^{13}C NMR (101 MHz, DMSO) δ 188.13, 163.95, 157.43, 154.55, 149.52, 143.95, 131.59, 130.63, 130.48, 130.15, 127.04, 126.70, 124.25, 123.05, 114.64, 109.09, 66.63, 56.10, 52.78. Purity was determined to be 99.5% by using HPLC. HRMS (ESI; *m/z*) calcd for C23H22N2O3, $[M+H]^+$, 375.1703; found 375.1713.

*4.1.6.8. (E)-3-(4-morpholinoquinolin-2-yl)-1-phenylprop-2-en-1-one (**14**).* Compound **5b** was reacted with compound **6b** according to general procedure to afford compound **14** as a yellow solid with a yield of 30%. ^{1}H NMR (400 MHz, $CDCl_3$) δ 8.21–8.09 (m, 4H), 8.01 (d, J = 8.4 Hz, 1H), 7.88 (d, J = 15.5 Hz, 1H), 7.74–7.67 (m, 1H), 7.64–7.59 (m, 1H), 7.56–7.49 (m, 3H), 7.11 (s, 1H), 4.01 (d, J = 4.4 Hz, 3H), 3.35–3.24 (m, 1H). ^{13}C NMR (101 MHz, $CDCl_3$) δ 190.82, 157.40, 153.88, 149.75, 144.17, 137.83, 133.09, 130.57, 129.81, 128.85, 128.70, 126.94, 126.23, 123.46, 123.27, 109.38, 66.91, 52.62. Purity was determined to be 98.8% by using HPLC. HRMS (ESI; *m/z*) calcd for C22H20N2O2, $[M+H]^+$, 345.1597; found 345.1609.

*4.1.6.9. (E)-1-(4-fluorophenyl)-3-(4-morpholinoquinolin-2-yl)prop-2-en-1-one (**15**).* Compound **5b** was reacted with compound **6c** according to general procedure to afford compound **15** as a yellow solid with a yield of 55%. ^{1}H NMR (400 MHz, $CDCl_3$) δ 8.23–8.10 (m, 4H), 8.03 (dd, J = 8.4, 0.9 Hz, 1H), 7.89 (d, J = 15.4 Hz, 1H), 7.72 (ddd, J = 8.4, 6.9, 1.4 Hz, 1H), 7.53 (ddd, J = 8.2, 6.9, 1.2 Hz, 1H), 7.22 (ddd, J = 8.7, 5.9, 2.4 Hz, 4H), 7.12 (s, 1H), 4.03 (d, J = 4.6 Hz, 1H), 3.30 (d, J = 4.6 Hz, 1H). ^{13}C NMR (101 MHz, $CDCl_3$) δ 189.05, 167.07, 164.53, 157.44, 153.72, 149.79, 144.24, 134.23 (d, J = 2.8 Hz), 131.46 (d, J = 9.3 Hz), 130.59, 129.81, 126.33 (d, J = 19.0 Hz), 123.46, 123.31, 115.82 (d, J = 21.8 Hz), 109.55, 66.90, 52.62. Purity was determined to be 100% by using HPLC. HRMS (ESI; *m/z*) calcd for C22H19FN2O2, $[M+H]^+$, 363.1503; found 363.1510.

*4.1.6.10. (E)-3-(4-morpholinoquinolin-2-yl)-1-(4-nitrophenyl)prop-2-en-1-one (**16**).* Compound **5b** was reacted with compound **6d** according to general procedure to afford compound **16** as a yellow solid with a yield of 62%. ^{1}H NMR (400 MHz, $CDCl_3$) δ 8.35 (d, J = 8.7 Hz, 2H), 8.23 (d, J = 8.7 Hz, 2H), 8.13 (d, J = 10.8 Hz, 1H), 8.11 (d, J = 3.6 Hz, 1H), 8.02 (d, J = 8.4 Hz, 1H), 7.90 (d, J = 15.4 Hz, 1H), 7.72 (t, J = 7.5 Hz, 1H), 7.54 (t, J = 7.6 Hz, 1H), 7.10 (s, 1H), 4.02 (d, J = 4.4 Hz, 4H), 3.29 (d, J = 4.4 Hz, 4H). ^{13}C NMR (101 MHz, $CDCl_3$) δ 189.25, 157.59, 153.11, 150.21, 149.73, 145.78, 142.56, 130.59, 129.99, 129.71, 126.51, 125.97, 123.89, 123.52, 123.38, 109.73, 66.87, 52.62. Purity was determined to be 99.6% by using HPLC. HRMS (ESI; *m/z*) calcd for C22H19N3O4, $[M+H]^+$, 390.1448; found 390.1458.

*4.1.6.11. (E)-1-(4-hydroxyphenyl)-3-(4-morpholinoquinolin-2-yl)prop-2-en-1-one (**17**).* Compound **5b** was reacted with compound **6e** according to general procedure to afford compound **17** as a yellow solid with a yield of 41%. ^{1}H NMR (400 MHz, DMSO) δ 10.50 (s, 1H), 8.26 (d, J = 15.6 Hz, 1H), 8.10 (d, J = 8.7 Hz, 2H), 8.07 (d, J = 8.4 Hz, 1H), 8.02 (d, J = 8.4 Hz, 1H), 7.78–7.71 (m, 2H), 7.60 (s, 1H), 7.57 (d, J = 7.3 Hz, 1H), 6.95 (d, J = 8.6 Hz, 2H), 3.91 (d, J = 4.0 Hz, 4H), 3.27 (d, J = 4.0 Hz, 5H). ^{13}C NMR (101 MHz, DMSO) δ 187.80, 163.00, 157.44, 154.66, 149.52, 143.55, 131.87, 130.66–130.50 (m), 130.15, 129.30, 127.16, 126.67, 124.25, 123.03, 116.03, 109.02, 66.64, 52.79. Purity was determined to be 98.6% by using HPLC. HRMS (ESI; *m/z*) calcd for C22H20N2O3, $[M+H]^+$, 361.1547; found 361.1558.

*4.1.6.12. (E)-1-(4-(benzyloxy)phenyl)-3-(4-morpholinoquinolin-2-yl) prop-2-en-1-one (**18**).* Compound **5b** was reacted with compound **6f** according to general procedure to afford compound **18** as a yellow solid with a yield of 74%. ^{1}H NMR (400 MHz, $CDCl_3$) δ 8.20–8.08 (m, 4H), 8.00 (d, J = 7.4 Hz, 1H), 7.87 (d, J = 15.4 Hz, 1H), 7.69 (t, J = 7.6 Hz,

1H), 7.54–7.33 (m, 6H), 7.09 (s, 2H), 7.06 (s, 1H), 5.16 (s, 2H), 4.01 (d, J = 4.4 Hz, 4H), 3.27 (d, J = 4.4 Hz, 4H). ^{13}C NMR (101 MHz, $CDCl_3$) δ 188.87, 162.82, 157.36, 154.08, 149.79, 143.29, 136.20, 131.23, 131.03, 130.56, 129.74, 128.73, 128.28, 127.54, 126.79, 126.11, 123.44, 123.25, 114.78, 109.51, 70.21, 66.92, 52.63. Purity was determined to be 99.3% by using HPLC. HRMS (ESI; *m/z*) calcd for C29H26N2O3, $[M+H]^+$, 451.2016; found 451.2026.

*4.1.6.13. (E)-3-(6-fluoro-4-morpholinoquinolin-2-yl)-1-(4-methoxyphenyl)prop-2-en-1-one (**19**)*. Compound **5c** was reacted with compound **6a** according to general procedure to afford compound **19** as a yellow solid with a yield of 52%. ^{1}H NMR (400 MHz, $CDCl_3$) δ 8.24–8.10 (m, 4H), 7.86 (d, J = 15.4 Hz, 1H), 7.62 (dd, J = 9.9, 2.8 Hz, 1H), 7.49 (ddd, J = 9.2, 8.0, 2.9 Hz, 1H), 7.14 (s, 1H), 7.02 (d, J = 8.9 Hz, 2H), 4.03 (d, J = 4.4 Hz, 4H), 3.92 (s, 3H), 3.26 (d, J = 4.4 Hz, 4H). ^{13}C NMR (101 MHz, $CDCl_3$) δ 188.72, 163.71, 161.66, 159.19, 156.99, 153.54, 146.77, 142.81, 133.06 (d, J = 9.3 Hz), 131.19, 126.81, 124.23 (d, J = 9.0 Hz), 120.02, 119.76, 113.93, 110.27, 107.25 (d, J = 23.4 Hz), 66.87, 55.53, 52.46. Purity was determined to be 99.8% by using HPLC. HRMS (ESI; *m/z*) calcd for C23H21FN2O3, $[M+H]^+$, 393.1609; found 393.1619.

*4.1.6.14. (E)-3-(6-fluoro-4-morpholinoquinolin-2-yl)-1-phenylprop-2-en-1-one (**20**)*. Compound **5c** was reacted with compound **6b** according to general procedure to afford compound **20** as a yellow solid with a yield of 62%. ^{1}H NMR (400 MHz, $CDCl_3$) δ 8.16–8.07 (m, 4H), 7.86 (d, J = 15.5 Hz, 1H), 7.67–7.58 (m, 2H), 7.57–7.43 (m, 3H), 7.13 (s, 1H), 4.01 (d, J = 4.4 Hz, 1H), 3.25 (d, J = 4.4 Hz, 1H). ^{13}C NMR (101 MHz, $CDCl_3$) δ 190.67, 161.73, 159.26, 157.00, 153.33, 146.81, 143.72, 137.80, 133.12, 128.82, 128.72, 126.94, 124.28 (d, J = 9.0 Hz), 119.98 (d, J = 25.6 Hz), 110.16, 107.28 (d, J = 23.4 Hz), 66.87, 52.46. Purity was determined to be 99.6% by using HPLC. HRMS (ESI; *m/z*) calcd for C22H19FN2O2, $[M+H]^+$, 363.1503; found 363.1513.

*4.1.6.15. (E)-3-(6-fluoro-4-morpholinoquinolin-2-yl)-1-(4-fluorophenyl) prop-2-en-1-one (**21**)*. Compound **5c** was reacted with compound **6c** according to general procedure to afford compound **21** as a yellow solid with a yield of 30%. ^{1}H NMR (400 MHz, $CDCl_3$) δ 8.22–8.09 (m, 4H), 7.86 (d, J = 15.4 Hz, 1H), 7.61 (dd, J = 9.8, 2.8 Hz, 1H), 7.54–7.43 (m, 1H), 7.20 (t, J = 8.6 Hz, 2H), 7.12 (s, 1H), 4.01 (d, J = 4.2 Hz, 4H), 3.26 (d, J = 4.2 Hz, 4H). ^{13}C NMR (101 MHz, $CDCl_3$) δ 188.90, 167.10, 164.57, 161.74, 159.27, 157.11, 153.11, 143.79, 134.15 (d, J = 2.9 Hz), 133.08 (d, J = 9.2 Hz), 131.47 (d, J = 9.3 Hz), 126.43, 124.33, 120.05 (d, J = 25.5 Hz), 115.86 (d, J = 21.9 Hz), 110.34, 107.30 (d, J = 23.4 Hz), 66.85, 52.46. Purity was determined to be 99.4% by using HPLC. HRMS (ESI; *m/z*) calcd for C22H18F2N2O2, $[M+H]^+$, 381.1409; found 381.1425.

*4.1.6.16. (E)-3-(6-fluoro-4-morpholinoquinolin-2-yl)-1-(4-nitrophenyl) prop-2-en-1-one (**22**)*. Compound **5c** was reacted with compound **6d** according to general procedure to afford compound **22** as a yellow solid with a yield of 37%. ^{1}H NMR (400 MHz, $CDCl_3$) δ 8.37 (d, J = 8.6 Hz, 2H), 8.24 (d, J = 8.5 Hz, 2H), 8.17–8.06 (m, 2H), 7.89 (d, J = 15.4 Hz, 1H), 7.62 (dd, J = 9.7, 2.3 Hz, 1H), 7.54–7.45 (m, 1H), 7.13 (s, 1H), 4.02 (d, J = 3.8 Hz, 4H), 3.26 (s, 4H). ^{13}C NMR (101 MHz, $CDCl_3$) δ 189.16, 161.89, 159.41, 157.22, 152.60, 150.27, 146.81, 145.45, 142.52, 133.21 (d, J = 9.1 Hz), 129.71, 125.91, 123.93, 120.22 (d, J = 25.7 Hz), 110.50, 107.36 (d, J = 23.4 Hz), 66.83, 52.46. Purity was determined to be 96.7% by using HPLC. HRMS (ESI; *m/z*) calcd for C22H18FN3O4, $[M+H]^+$, 408.1354; found 408.1364.

*4.1.6.17. (E)-3-(6-fluoro-4-morpholinoquinolin-2-yl)-1-(4-hydroxyphenyl)prop-2-en-1-one (**23**)*. Compound **5c** was reacted with compound **6e** according to general procedure to afford compound **23** as a yellow solid with a yield of 32%. ^{1}H NMR (400 MHz, DMSO) δ 10.51 (s, 1H), 8.26 (d, J = 15.6 Hz, 1H), 8.10 (d, J = 8.0 Hz, 3H), 7.84–7.62 (m, 4H), 6.95 (d, J = 7.7 Hz, 2H), 3.91 (d, J = 6.0 Hz, 4H), 3.21 (d, J = 6.0 Hz, 4H). ^{13}C NMR (101 MHz, DMSO) δ 187.25, 162.50, 156.64, 153.83, 146.15, 142.72, 132.94, 131.36, 128.78, 126.76, 123.63, 119.79, 115.52, 109.37, 107.55, 107.32, 66.09, 52.11. Purity was determined to be 95.4% by using HPLC. HRMS (ESI; *m/z*) calcd for C22H19FN2O3, $[M+H]^+$, 379.1452; found 379.1464.

*4.1.6.18. (E)-1-(4-(benzyloxy)phenyl)-3-(6-fluoro-4-morpholinoquinolin-2-yl)prop-2-en-1-one (**24**)*. Compound **5c** was reacted with compound **6f** according to general procedure to afford compound **24** as a yellow solid with a yield of 79%. ^{1}H NMR (400 MHz, $CDCl_3$) δ 8.18–8.06 (m, 4H), 7.85 (d, J = 15.4 Hz, 1H), 7.61 (dd, J = 9.9, 2.8 Hz, 1H), 7.53–7.33 (m, 6H), 7.12 (s, 1H), 7.08 (d, J = 8.8 Hz, 2H), 5.17 (s, 2H), 4.01 (d, J = 4.4 Hz, 4H), 3.25 (d, J = 4.4 Hz, 4H). ^{13}C NMR (101 MHz, $CDCl_3$) δ 188.76, 162.85, 153.56, 146.81, 142.90, 136.18, 133.13, 133.04, 131.19, 130.99, 128.72, 128.28, 127.51, 126.78, 124.21, 120.01, 119.75, 114.80, 110.27, 107.24 (d, J = 23.6 Hz), 70.22, 66.87, 52.46. Purity was determined to be 96.0% by using HPLC. HRMS (ESI; *m/z*) calcd for C29H25FN2O3, $[M+H]^+$, 469.1921; found 469.1927.

*4.1.6.19. (E)-1-(4-methoxyphenyl)-3-(4-morpholino-6-nitroquinolin-2-yl) prop-2-en-1-one (**25**)*. Compound **5d** was reacted with compound **6a** according to general procedure to afford compound **25** as a yellow solid with a yield of 31%. ^{1}H NMR (400 MHz, DMSO) δ 8.80 (d, J = 2.4 Hz, 1H), 8.41 (dd, J = 9.2, 2.4 Hz, 1H), 8.34 (d, J = 15.6 Hz, 1H), 8.17 (dd, J = 9.0, 5.2 Hz, 3H), 7.77 (s, 1H), 7.73 (s, 1H), 7.14 (d, J = 8.8 Hz, 2H), 3.94 (t, J = 8.4 Hz, 4H), 3.89 (s, 3H), 3.38 (t, J = 8.5 Hz, 4H). ^{13}C NMR (101 MHz, $CDCl_3$) δ 188.35, 163.92, 159.14, 157.36, 152.12, 144.64, 141.77, 132.05, 131.25, 130.57, 128.64, 123.21, 122.05, 120.79, 114.03, 111.07, 66.66, 55.57, 52.85. Purity was determined to be 98.5% by using HPLC. HRMS (ESI; *m/z*) calcd for C23H21N3O5, $[M+H]^+$, 420.1554; found 420.1567.

*4.1.6.20. (E)-3-(4-morpholino-6-nitroquinolin-2-yl)-1-phenylprop-2-en-1-one (**26**)*. Compound **5d** was reacted with compound **6b** according to general procedure to afford compound **26** as a yellow solid with a yield of 33%. ^{1}H NMR (400 MHz, $CDCl_3$) δ 8.91 (s, 1H), 8.50–8.39 (m, 1H), 8.26–8.07 (m, 4H), 7.82 (d, J = 15.4 Hz, 1H), 7.67–7.49 (m, 13H), 7.17 (s, 1H), 4.04 (s, 4H), 3.35 (s, 4H). ^{13}C NMR (101 MHz, $CDCl_3$) δ 193.51, 159.72, 155.46, 155.44, 151.81, 145.93, 145.89, 133.42, 132.89, 128.87, 128.82, 123.93, 123.48, 120.94, 120.82, 105.75, 66.56, 52.83. Purity was determined to be 99.9% by using HPLC. HRMS (ESI; *m/z*) calcd for C22H19N3O4, $[M+H]^+$, 390.1448; found390.1458.

*4.1.6.21. (E)-1-(4-fluorophenyl)-3-(4-morpholino-6-nitroquinolin-2-yl) prop-2-en-1-one (**27**)*. Compound **5d** was reacted with compound **6c** according to general procedure to afford compound **27** as a yellow solid with a yield of 35%. ^{1}H NMR (400 MHz, $CDCl_3$) δ 8.94 (d, J = 2.0 Hz, 1H), 8.45 (dd, J = 9.2, 2.1 Hz, 1H), 8.31–8.12 (m, 4H), 7.85 (d, J = 15.3 Hz, 1H), 7.23 (dd, J = 16.9, 8.4 Hz, 2H), 7.15 (s, 1H), 4.06 (d, J = 3.8 Hz, 4H), 3.36 (s, 4H). ^{13}C NMR (101 MHz, $CDCl_3$) δ 188.56, 167.26, 164.72, 159.25, 156.96, 152.10, 144.73, 142.76, 133.94, 132.11, 131.53 (d, J = 9.4 Hz), 128.17, 123.31, 122.11, 120.81, 115.99 (d, J = 21.9 Hz), 111.14, 66.64, 52.86. Purity was determined to be 98.9% by using HPLC. HRMS (ESI; *m/z*) calcd for C22H18FN3O4, $[M+H]^+$, 408.1354; found 408.1366.

*4.1.6.22. (E)-3-(4-morpholino-6-nitroquinolin-2-yl)-1-(4-nitrophenyl) prop-2-en-1-one (**28**)*. Compound **5d** was reacted with compound **6d** according to general procedure to afford compound **28** as a yellow solid with a yield of 30%. ^{1}H NMR (400 MHz, $CDCl_3$) δ 8.95 (d, J = 2.5 Hz, 1H), 8.47 (dd, J = 9.3, 2.5 Hz, 1H), 8.41 (dd, J = 6.9, 1.9 Hz, 2H), 8.27 (ddd, J = 26.3, 8.9, 5.7 Hz, 4H), 7.90 (d, J = 15.4 Hz, 1H), 7.24 (s, 1H), 4.08 (d, J = 4.4 Hz, 4H), 3.41 (d, J = 4.4 Hz, 4H). ^{13}C NMR (101 MHz,

$CDCl_3$) δ 189.03, 159.40, 156.43, 151.82, 150.36, 144.75, 144.09, 142.05, 131.72, 129.75, 127.75, 123.92, 123.44, 122.07, 120.77, 111.09, 66.52, 52.69. Purity was determined to be 95.3% by using HPLC. HRMS (ESI; *m/z*) calcd for C22H18N4O6, $[M+H]^+$, 435.1299; found 435.1311.

*4.1.6.23. (E)-1-(4-hydroxyphenyl)-3-(4-morpholino-6-nitroquinolin-2-yl) prop-2-en-1-one **(29)***. Compound **5d** was reacted with compound **6e** according to general procedure to afford compound **29** as a yellow solid with a yield of 34%. ^{1}H NMR (400 MHz, DMSO) δ 10.56 (s, 1H), 8.80 (d, J = 2.5 Hz, 1H), 8.41 (dd, J = 9.2, 2.5 Hz, 1H), 8.34 (d, J = 15.6 Hz, 1H), 8.16 (d, J = 9.2 Hz, 1H), 8.10 (d, J = 8.7 Hz, 2H), 7.74 (d, J = 10.8 Hz, 1H), 6.95 (d, J = 8.7 Hz, 2H), 3.93 (t, J = 4.0 Hz, 4H), 3.55–3.23 (m, 4H). ^{13}C NMR (101 MHz, DMSO) δ 187.14, 162.69, 158.62, 157.52, 151.43, 144.12, 142.02, 131.61, 131.50, 128.65, 128.54, 123.05, 121.32, 120.89, 115.61, 110.20, 66.01, 52.45. Purity was determined to be 96.2% by using HPLC. HRMS (ESI; *m/z*) calcd for C22H19N3O5, $[M+H]^+$, 406.1397; found 406.1409.

*4.1.6.24. (E)-1-(4-(benzyloxy)phenyl)-3-(4-morpholino-6-nitroquinolin-2-yl)prop-2-en-1-one **(30)***. Compound **5d** was reacted with compound **6f** according to general procedure to afford compound **30** as a yellow solid with a yield of 69%. ^{1}H NMR (400 MHz, DMSO) δ 8.81 (d, J = 2.3 Hz, 1H), 8.42 (dd, J = 9.2, 2.3 Hz, 1H), 8.36 (d, J = 15.6 Hz, 1H), 8.18 (dd, J = 9.0, 3.7 Hz, 3H), 7.76 (d, J = 14.9 Hz, 2H), 7.50 (d, J = 7.2 Hz, 2H), 7.43 (t, J = 7.3 Hz, 2H), 7.37 (t, J = 7.2 Hz, 1H), 7.22 (d, J = 8.7 Hz, 2H), 5.27 (s, 2H), 3.92 (d, J = 5.0 Hz, 4H), 3.40 (t, 4H). ^{13}C NMR (101 MHz, $CDCl_3$) δ 188.38, 163.06, 159.15, 157.34, 152.10, 144.66, 141.77, 136.10, 132.03, 131.26, 130.90, 130.76, 128.74, 128.31, 127.50, 123.23, 122.05, 120.78, 114.89, 111.05, 70.26, 66.65, 52.85. Purity was determined to be 95.4% by using HPLC. HRMS (ESI; *m/z*) calcd for C29H25N3O5, $[M+H]^+$, 496.1876; found 496.1867.

*4.1.7. General procedure for the preparation of 3-hydroxy-3-(6-substituted −4-morpholinoquinolin-2-yl)-1-(4-substituted-phenyl)propan-1-ones **(31–33)***

To a solution of 1-(4-substituted-phenyl)ethanone (**6d, 6f**, 1.84 mmol, 1.2 equiv) in 10 mL EtOH, was added aldehyde (**5a–b,** 1.54 mmol), followed with 1% NaOH (0.5 mL). The reaction was stirred at room temperature, and monitored by using TLC. The reaction mixture was quenched with NH_4Cl solution. The organic layer was extracted with ethyl acetate (3 × 10 mL). The combined organic layer was washed with brine for three times, dried over anhydrous sodium sulfate, filtered, concentrated, and the residue was purified by using silica gel chromatograph with dichloromethane/MeOH (100/1–20/1) to give compound **31–33**.

*4.1.7.1. 3-hydroxy-3-(6-methoxy-4-morpholinoquinolin-2-yl)-1-(4-nitrophenyl)propan-1-one **(31)***. Compound **5a** was reacted with compound **6d** according to general procedure to afford compound **31** as a yellow solid with a yield of 70%. ^{1}H NMR (400 MHz, $CDCl_3$) δ 8.29 (d, J = 8.8 Hz, 2H), 8.14 (d, J = 8.8 Hz, 2H), 7.87 (d, J = 9.1 Hz, 1H), 7.33 (dd, J = 9.1, 2.8 Hz, 1H), 7.27 (d, J = 1.6 Hz, 1H), 7.05 (s, 1H), 5.47 (dd, J = 7.4, 4.3 Hz, 1H), 4.75 (s, 1H), 3.99 (t, J = 4.6 Hz, 4H), 3.93 (s, 3H), 3.59 (qd, J = 16.6, 5.9 Hz, 2H), 3.23 (d, J = 4.6 Hz, 4H). ^{13}C NMR (101 MHz, $CDCl_3$) δ 198.29, 159.02, 157.27, 156.71, 150.39, 143.85, 141.53, 130.83, 129.42, 123.81, 123.59, 121.37, 106.31, 102.29, 70.35, 66.91, 55.50, 52.38, 46.91. Purity was determined to be 99.2% by using HPLC. HRMS (ESI; *m/z*) calcd for C23H23N3O6, $[M+H]^+$, 438.1659; found 438.1664.

*4.1.7.2. 1-(4-(benzyloxy)phenyl)-3-hydroxy-3-(6-methoxy-4-morpholinoquinolin-2-yl)propan-1-one **(32)***. Compound **5a** was reacted with compound **6f** according to general procedure to afford compound **32** as a yellow solid with a yield of 84%. ^{1}H NMR (400 MHz, $CDCl_3$) δ 7.89 (d, J = 8.9 Hz, 2H), 7.84 (d, J = 9.1 Hz, 1H), 7.32 (q, J = 7.9 Hz, 4H), 7.26 (ddd, J = 11.8, 6.7, 2.3 Hz, 2H), 7.22–7.18 (m, 1H), 7.02 (s, 1H), 6.91 (d, J = 8.9 Hz, 2H), 5.38 (dd, J = 7.6, 4.2 Hz, 1H), 5.04 (s, 2H), 3.90 (t, J = 4.5 Hz, 4H), 3.85 (s, 3H), 3.43 (qd, J = 16.8, 6.0 Hz, 2H), 3.24–3.03 (m, 4H). ^{13}C NMR (101 MHz, $CDCl_3$) δ 198.50, 162.94, 160.06, 157.10, 156.46, 144.10, 136.10, 130.97, 130.71, 130.26, 128.72, 128.29, 127.50, 123.53, 121.15, 114.62, 106.48, 102.22, 70.67, 70.17, 66.96, 55.49, 52.37, 45.95. Purity was determined to be 99.4% by using HPLC. HRMS (ESI; *m/z*) calcd for C30H30N2O5, $[M+H]^+$, 499.2227; found 499.2235.

*4.1.7.3. 1-(4-(benzyloxy)phenyl)-3-hydroxy-3-(4-morpholinoquinolin-2-yl)propan-1-one **(33)***. Compound **5b** was reacted with compound **6f** according to general procedure to afford compound **33** as a yellow solid with a yield of 79%. ^{1}H NMR (400 MHz, $CDCl_3$) δ 8.05–7.96 (m, 4H), 7.68 (ddd, J = 8.5, 6.9, 1.3 Hz, 1H), 7.56–7.33 (m, 6H), 7.12 (s, 1H), 7.06–6.99 (m, 2H), 5.50 (dd, J = 7.6, 4.2 Hz, 1H), 5.15 (s, 2H), 4.01 (t, J = 4.6 Hz, 4H), 3.54 (qd, J = 16.8, 6.0 Hz, 2H), 3.37–3.18 (m, 4H). ^{13}C NMR (101 MHz, $CDCl_3$) δ 198.40, 162.95, 162.52, 157.52, 148.40, 136.12, 130.70, 130.28, 129.56, 129.33, 128.71, 128.27, 127.47, 125.25, 123.51, 122.62, 114.64, 105.84, 70.75, 70.18, 66.92, 52.65, 45.94. Purity was determined to be 99.4% by using HPLC. HRMS (ESI; *m/z*) calcd for C29H28N2O4, $[M+H]^+$, 469.2122; found 469.2127.

*4.1.8. General procedure for the preparation of 3-morpholino-N-((4-morpholinoquinolin-2-yl)methyl)propan-1-amine **(34)***

To a solution of 3-morpholinopropan-1-amine (59.5 mg, 0.41 mmol) in 5 mL trichloromethane, was added 4-morpholinoquinoline-2-carbaldehyde (**5b,** 50.0 mg, 0.21 mmol) and $NaBH_3CN$ (52.0 mg, 0.83 mmol), followed with HAc (61.9 mg, 1.03 mmol). The mixture was stirred at room temperature, and monitored by using TLC. The reaction mixture was quenched with saturated sodium bicarbonate solution. The organic layer was extracted with dichloromethane (3 × 5 mL). The combined organic layers were washed with brine for three times, dried over anhydrous sodium sulfate, filtered, concentrated, and the residue was purified by using silica gel chromatograph with dichloromethane/MeOH (50/1–20/1) to give desired compound **34** as a colorless liquid with a yield of 43%. ^{1}H NMR (400 MHz, $CDCl_3$) δ 7.99 (dd, J = 8.4, 1.0 Hz, 1H), 7.96–7.91 (m, 1H), 7.66 (ddd, J = 8.4, 6.9, 1.4 Hz, 1H), 7.49 (ddd, J = 8.2, 6.9, 1.1 Hz, 1H), 6.91 (s, 1H), 4.26 (s, 2H), 3.97 (d, J = 4.6 Hz, 4H), 3.73 (t, J = 4.6 Hz, 4H), 3.25 (d, J = 4.4 Hz, 4H), 3.15 (t, J = 6.0 Hz, 2H), 2.72–2.48 (m, 6H), 2.07–1.83 (m, 2H). ^{13}C NMR (101 MHz, $CDCl_3$) δ 157.72, 155.06, 148.90, 129.78, 129.15, 125.65, 123.78, 122.58, 107.63, 66.80, 66.70, 57.93, 53.62, 53.23, 52.56, 49.37, 23.19. Purity was determined to be 100% by using HPLC. HRMS (ESI; *m/z*) calcd for C21H30N4O2, $[M+H]^+$, 371.2393; found 371.2420.

*4.1.9. General procedure for the preparation of (E)-6-methoxy-2-(3-(4-methoxyphenyl)-3-oxoprop-1-en-1-yl)-1-methyl-4-morpholinoquinolin-1-ium iodide **(35)***

To a solution of compound **7** (30 mg, 0.074 mmol) in THF (5 mL), was added methyl iodide (21.1 mg, 0.148 mmol). The reaction mixture was stirred in sealed tube at 80 °C for two days. After cooled to room temperature and filtered, the solid was washed with THF to give the desired compound (**35**) as a yellow solid with a yield of 35%. ^{1}H NMR (400 MHz, DMSO) δ 8.32 (d, J = 9.7 Hz, 1H), 8.25–8.14 (m, 3H), 7.98 (d, J = 15.4 Hz, 1H), 7.75 (dd, J = 9.7, 2.8 Hz, 1H), 7.59 (s, 1H), 7.42 (d, J = 2.8 Hz, 1H), 7.16 (d, J = 9.0 Hz, 2H), 4.22 (s, 3H), 4.00 (s, 3H), 3.94–3.81 (m, 11*H*). ^{13}C NMR (101 MHz, DMSO) δ 187.02, 164.48, 159.43, 157.60, 150.71, 136.36, 134.65, 134.19, 132.06, 129.80, 125.49, 121.87, 121.75, 114.83, 107.59, 106.49, 66.24, 56.51, 56.24, 52.36. Purity was determined to be 95.5% by using HPLC. HRMS (ESI; *m/z*) calcd for C25H27IN2O4, $[M-I]^+$, 419.1965; found 419.1956.

*4.1.10. General procedure for the preparation of 1-(4-hydroxyphenyl)-3-(6-methoxy-4-morpholinoquinolin-2-yl)propan-1-one (**36**) and 1-(4-(benzyloxy)phenyl)-3-(6-methoxy-4-morpholinoquinolin-2-yl)propan-1-one (**37**)*

To a solution of compound **12** (60 mg, 0.125 mmol) in ethyl acetate (10 mL), was added Pd/C (5%, 5.0 mg). The reaction mixture was stirred at hydrogen atmosphere for 20 mins. The mixture was filtered, the filtrate was concentrated under reduced pressure, and the residue was purified by using silica gel chromatograph with dichloromethane/MeOH (100/1–50/1) to give compound **36–37**.

*4.1.10.1. 1-(4-hydroxyphenyl)-3-(6-methoxy-4-morpholinoquinolin-2-yl) propan-1-one (**36**).* The compound was obtained as a white solid with a yield of 35%. ^{1}H NMR (400 MHz, $CDCl_3$) δ 8.02 (d, J = 8.3 Hz, 1H), 7.59 (d, J = 8.7 Hz, 2H), 7.35–7.29 (m, 2H), 6.99 (s, 1H), 6.76 (d, J = 8.8 Hz, 2H), 4.02 (d, J = 4.4 Hz, 4H), 3.94 (s, 3H), 3.39 (t, J = 6.5 Hz, 2H), 3.36–3.28 (m, 6H). Purity was determined to be 99.1% by using HPLC. HRMS (ESI; *m/z*) calcd for C23H24N2O4, $[M+H]^+$, 393.1764; found 393.1820.

*4.1.10.2. 1-(4-(benzyloxy)phenyl)-3-(6-methoxy-4-morpholinoquinolin-2-yl)propan-1-one (**37**).* The compound was obtained as a white solid with a yield of 41%. ^{1}H NMR (400 MHz, $CDCl_3$) δ 8.02 (d, J = 8.9 Hz, 2H), 7.92 (d, J = 9.0 Hz, 1H), 7.49–7.35 (m, 5H), 7.30 (dt, J = 7.8, 2.4 Hz, 2H), 7.02 (d, J = 8.9 Hz, 2H), 6.88 (s, 1H), 5.15 (s, 2H), 4.00 (d, J = 4.6 Hz, 4H), 3.94 (s, 3H), 3.55 (t, J = 7.2 Hz, 2H), 3.36 (t, J = 7.2 Hz, 2H), 3.22 (d, J = 4.6 Hz, 4H). ^{13}C NMR (101 MHz, $CDCl_3$) δ 198.11, 162.55, 159.38, 156.75, 155.85, 136.24, 130.78, 130.43, 130.40, 128.69, 128.22, 127.47, 122.81, 120.78, 114.54, 109.87, 102.21, 70.13, 66.99, 55.46, 52.37, 37.52, 32.97. Purity was determined to be 95.6% by using HPLC. HRMS (ESI; *m/z*) calcd for C30H30N2O4, $[M+H]^+$, 483.2278; found 483.2297.

4.2. Biochemicals and materials

All oligomers/primers used in this study were purchased from Invitrogen or Sangon, as shown in Table S1 in Supporting Information. Stock solutions of all the derivatives (10 mM) were prepared using DMSO (10%) or double-distilled deionized water. Further dilutions to working concentrations were carried out with double-distilled deionized water or buffer. All other chemicals or solvents were of analytical grade or better.

4.3. Expression and purification of recombinant hnRNP K

hnRNP K was expressed as 6×His-tagged fusion protein in *Escherichia coli* strain BL21 (DE3) and purified to homogeneity by using affinity chromatography, as described previously [32]. The purified hnRNP K protein was stored in the following buffer: 10 mM Na_3PO_4, 500 mM NaCl, 0.05% Tween-20, 5 mM β-mercaptoethanol, pH 7.0.

4.4. Electrophoretic mobility shift assay (EMSA)

The binding study of hnRNP K with 5 μM 5′-FAM labeled Py33 oligonucleotide was carried out by using EMSA. Protein and Py33 component were mixed in a 10 μL reaction volume, incubated at 37 °C for 1 h, and loaded on 8% native PAGE at 4 °C and 10 V·cm^{-1} in 0.5 × TBE buffer (Tris/borate). The binding buffer consists of 20 mM Tris, 100 mM NaCl, 1 mM EDTA, 0.1 mM dithiothreitol, 5% glycerol (v/v), 1 mg/mL BSA, pH 6.0. For displacement experiment, a final concentration of 10 μM hnRNP K was pre-incubated with different concentration of compound for 1 h at 37 °C, before addition of 5 μM 5′-FAM-labeled oligonucleotide. The mixtures were incubated for 30 mins, and loaded on 8% native PAGE under the same condition as shown above.

4.5. Filter binding assay

Filter binding assays were performed as described previously [54]. In brief, a DEAE membrane was placed directly below the nitrocellulose membrane to trap any DNA not retained by the nitrocellulose. The two membranes were positioned on a 96-well dot-blot apparatus. The nitrocellulose membrane was treated with 0.5 M KOH for 10 min at 4 °C and washed with 1 × binding buffer (10 mM Tris HCl, pH 7.4) prior to use. Increasing concentrations of the recombinant hnRNP K protein and the indicated DNA substrate were mixed in 20 μL buffer (10 mM Tris HCl, pH 6.0) and incubated for 30 min at 37 °C. A 15 μL aliquot was applied to a nitrocellulose filter under vacuum and washed twice with 200 μL of 1 × binding buffer. The nitrocellulose and DEAE filters were dried, and the bound and unbound radioactivity were quantified by using Phosphor Imager analysis.

4.6. Surface plasmon resonance (SPR) measurement

SPR measurement was performed on a ProteOn XPR36 Protein Interaction Array system (Bio-Rad Laboratories, Hercules, CA) using a Neutravidin-coated GLH sensor chip. For immobilization, in a typical experiment, the chips were activated simultaneously by injecting 200 μL of a freshly mixed solution of EDAC and SulfoNHS. Immediately after activation, 200 μL of hnRNP K protein (50 μg/mL in sodium acetate, pH 4.5) was injected into the channels. For deactivation, 150 μL of ethanolamine hydrochloride (1 M, pH 8.5) was injected into the relevant channels simultaneously. The protein was immobilized (~10,000 RU) in channel 1, and a blank cell was set as a control. Ligand solutions (at 0, 1.875, 3.73, 7.5, 15, 30 μM) were prepared with the running buffer (50 mM Na_3PO_4, 500 mM NaCl, 0.005% Tween-20, pH 7.0) through serial dilutions from stock solution (10 mM in DMSO). Six concentrations were injected simultaneously at a flow rate of 25 μL/min for 200 s of association phase, followed with 300 s of dissociation phase. The GLH sensor chip was regenerated with short injection of 50 mM NaOH between consecutive measurements. The final graphs were obtained by subtracting blank sensorgrams from protein sensorgrams. Data were analyzed with ProteOn manager software.

4.7. Microscale thermophoresis experiment (MST)

MST measurements were performed by using a Nano Temper Monolith NT.115 instrument (Nano Temper Technologies GmbH). Briefly, purified hnRNP K was labeled with the Monolith NT™ Protein Labeling Kit RED (Cat#L001) according to the supplied labeling protocol. Labeled hnRNP K and DNA (Table S1) were used at a concentration of 200 nM. The compounds were titrated in 1:1 dilutions beginning at 50 μM, which contained 2.5% DMSO. Samples were diluted in binding buffer supplemented with DMSO at a final concentration of 2.5% to make sure that all samples contained the same DMSO concentration. The samples were incubated for 10 min and measured at an IRlaser power of 20% and a LED power of 40% with a laser-on time of 30 s and a laser-off time of 5 s. All measurements were made at least three times.

4.8. CD experiments

CD experiments were performed on a Chirascan circular dichroism spectrophotometer (Applied Photophysics). A quartz cuvette with 4 mm path length was used for the spectra recorded over a wavelength range of 230–350 nm at 1 nm bandwidth, 1 nm step size, and 0.5 s per point. The oligomer *c-myc* Py33 (Table S1) was diluted from stock to the required concentration (5 μM) with the binding buffer (pH 6.0). Then annealed by heating at 95 °C for 5 min, gradually cooled to room temperature, and stored at 4 °C overnight. Then the oligomer solution was mixed with hnRNP K protein. Spectra were recorded for three times over a wavelength range of 230–350 nm, averaged, smoothed, and

baseline corrected to remove signal contribution from buffer. Final analysis of the data was carried out using Origin 8.0 (OriginLab Corp.).

4.9. Fluorescence resonance energy transfer (FRET) assays

FRET assays were performed on a Fluoromax-4 fluorescence spectrophotometer (HORIBA, USA). A quartz cuvette with a 2 mm × 10 mm path length was used for spectral recording at 5 nm excitation and emission slit widths unless otherwise specified. The dual fluorescently labeled oligonucleotide Py33 (Table S1) was used in the assays, in which 6-carboxyfluorescein (FAM) was used as a donor fluorophore and 6-carboxytetramethylrhodamine (TAMRA) as an acceptor fluorophore. The oligonucleotide was first prepared by heating at 95 °C for 5 min followed by slowly cooling to room temperature and stored at 4 °C overnight. Small aliquots of a stock solution of hnRNP K protein or compound **25** were added into the solution containing DNA at a fixed concentration (50 nM) at pH 6.0. After each addition of sample, the reaction was stirred and allowed to equilibrate for at least 1 min, and the fluorescence measurement was recorded at excitation wave (480 nm).

4.10. Cell culture

Human cervical cancer cell line Siha, human lung adenocarcinoma cell line A549, human squamous cervical cancer cell line Hela, human leukemia cancer cell HL60, human bone osteosarcoma epithelial cell line U2OS, human melanoma cell line A375, human hepatocellular carcinoma cell line HuH7, and human embryonic kidney cell line HEK293 were purchased from China Center for Type Culture Collection in Wuhan. The cell lines were maintained in RPMI-1640 or DMEM medium supplemented with 10% fetal calf serum at 37 °C in a humidified atmosphere with 5% CO_2.

4.11. MTT cytotoxicity assay

Siha, A549, Hela, U2OS, A375, HuH7, and HEK293 cells were seeded on 96-well plates (5.0×10^3 per well) with 100 μL of culture medium and incubated for 12 h at 37 °C in a humidified atmosphere with 5% CO_2, respectively. After the cells were incubated in the presence or absence of the indicated concentrations of compound **25** for 48 h and the control group was administered the same volume of DMSO, 20 μL of 2.5 mg/mL methyl thiazolyl tetrazolium (MTT) solution was added to each well and further incubated for 4 h. The cells in each well were then treated with dimethyl sulfoxide (200 μL) after the culture medium was siphoned off and the absorbance was recorded at 570 nm. All drug doses were parallel tested in triplicate, and the cytotoxicity was evaluated based on the percentage of cell survival in a dose dependent manner regarding to the negative control. The final IC_{50} values were calculated by using the Graph Pad Prism 5.

4.12. Chromatin immunoprecipitation (ChIP)

ChIP experiments were performed using a Magna ChIP™ Kit (Millipore) following the manufacturer's protocol with all buffers used included in the kit. Hela cells were fixed with 1% formaldehyde for 10 min and then lysed. Chromatin was sheared to an average size of 0.2–0.5 kb using a SCIENTZ-II D sonicator (SCI-ENTZ, China). Then 10% of the lysate was removed for use as an input, and 2 μg of antibody against hnRNP K (ab39975, Abcam) was used for ChIP. Normal rabbit IgG (sc-3888, SantaCruz) was used as a negative control. ChIP was performed overnight at 4 °C, and immune complexes were collected using the protein A magnetic beads provided in the kit. After extensive washing with a buffer provided in the kit, the DNA was extracted from immunoprecipitated chromatin and amplified by using PCR with *Chip c-myc S* and *Chip c-myc A* primers (Table S1).

4.13. Molecular docking studies

KH3 domain of hnRNP-K (KH3_hnRNP-K) protein was downloaded from Protein Data Bank (PDBID: 1ZZI). The protein structure was cleaned, inspected for errors and missing residues, hydrogens were added, and the water molecules and the ligand were deleted. Compound **25** to be modeled was constructed and optimized by using ChemDraw and saved in SDF file format, and was corrected by using MOE software. Hydrogens were added, and the ligand was minimized with the conjugate gradient method using the MMFF94x force field with MMFF94 charges, a distance-dependent dielectric function, and a 0.01 kcal mol^{-1} $Å^{-1}$ energy gradient convergence criterion. SsDNA binding site on KH3_hnRNP-K was defined as the site of ligand binding over KH3_hnRNP-K and the ligand was docked at the defined binding site using MOE. Induced fit was used for docking with the default parameters. The top 30 docking poses of the ligand were inspected visually following the docking runs. The highest-ranked pose for compound **25** was merged into the crystal structure. Energy minimization was performed for the highest-ranked pose of compound **25**. The AMBER forcefield was utilized within the MOE software for energy minimization.

4.14. RNA extraction and RT-PCR

Hela cells were seeded in 6-well plate (2×10^5 cells/well), and incubated for 12 h at 37 °C in a humidified atmosphere with 5% CO_2. After the cells were incubated in the presence or absence of different concentrations of compound **25** and the control group was administered the same volume of DMSO for 3 h, the harvested cells were washed with 1 × PBS (pH 7.4) and lysed in a TRIzol solution. The total RNA was extracted according to the protocol supplied by the Takara Company and eluted in distilled, deionized water with 0.1% diethyl pyrocarbonate (DEPC) to a final volume of 30 μL. RNA was quantified spectrophotometrically. The total RNA was used as a template for reverse transcription according to the following protocol: each 20 μL reaction contained 1 × M-MLV buffer, 500 μM dNTP, 100 pmol oligo dT18 primer, 100 units of M-MLV reverse transcriptase, DEPC-H_2O, and 1.5 μg total RNA. The mixtures were incubated at 42 °C for 60 min for reverse transcription, then at 70 °C for 15 min. PCR was performed according to the following protocol: each 20-μL reaction contained 1 × PCR buffer, 500 μM dNTPs, 0.2 μM primer pairs, 1 unit *Taq* polymerase, 0.1% DEPC-H_2O and 2 μL cDNA template. The reactions were incubated in a Master-cycler Personal (Eppendorf) according to the following protocol: 95 °C for 5 min, 30 cycles of 95 °C for 1 min, 58 °C for 30 s and 72 °C for 1 min. The amplified products were separated on a 1.2% agarose gel, and the gel was photographed using a Gel Doc 2000 Imager System.

4.15. Western blot

After Hela cells were taken board for each well of 2×10^5 and then treated with different concentrations of compound **25** for 48 h, the cells harvested from each well of culture plates were lysed in 200 μL of protein extraction buffer consisting of 1 mM PMSF for 30 min. The suspension was centrifuged at 10,000 rpm at 4 °C for 15 min, and the protein content of supernatant was measured by using BCA assay. The same amount of protein for each sample was loaded onto 8% polyacrylamide gel, and then transferred to a microporous polyvinylidene difluoride (PVDF) membrane. Western blotting was performed by using anti-c-MYC and anti-β-actin (cell signaling technology) antibodies, as well as horseradish peroxidase-conjugated anti-rabbit secondary antibody. Protein bands were visualized by using chemiluminescence substrate.

4.16. Colony formation assay

Hela cells were subsequently seeded in 6-well culture plates (1000/well) for a 24 h pre-culture at 37 °C in a humidified atmosphere with 5% CO_2, then treated with compound **25** at different concentrations for 9 days. The cells were washed with 1 × PBS and fixed with ice cold methanol for 10 min, followed by the addition of 0.5% crystal violet solution for 30 min to observe the colony formation. Finally, the plates were washed with water, dried and photographed.

4.17. Wound-scratch assay

The cells were grown in a monolayer and a cross-shaped scrape was made through the confluent monolayers using a plastic pipette tip. Cells were washed a few times with PBS to remove cell debris, and a fresh medium was added. The time of scratching wound was designated as time 0 h. Several wounded areas were noted for orientation, observed and photographed using phase-contrast microscopy after scratching for 24 h.

4.18. Annexin V-FITC apoptosis detection

An annexin V-FITC apoptosis detection kit was purchased from eBioscience Inc. (San Diego, CA) and was used to study apoptosis induced by the synthesized compounds. This study was performed according to the instructions provided by the manufacturer. Hela cells were treated with compound **25** at the IC_{50} dose for 24 h prior to harvesting. The cells were resuspended in annexin V-FITC containing binding buffer. After incubation at room temperature for 30 min, the cells were washed and resuspended with PI and subjected to flow cytometric analysis (FAC Scan flow cytometer; Becton Dickinson, San Jose, CA).

4.19. Evaluation of in vivo antitumor activity

BALB/c female nude mice (five weeks old) were purchased from and housed at the Experimental Animal Center of Sun Yat-sen University (Guangzhou, China) and maintained in pathogen-free conditions (12 h light-dark cycle at 24 ± 1 °C with 60–70% humidity and provided with food and water ad libitum). All procedures were approved by the Animal Care and Use Committee of Sun Yat-sen University and conformed to the legal mandates and national guidelines for the care and maintenance of laboratory animals. Hela cells were harvested, pelleted through centrifugation at 800g for 5 min, and resuspended in sterile serum-free medium without EDTA. The cells (1×10^7 in 100 μL) were then subcutaneously implanted into the underarm regions of three mice. After the tumors grew to almost 1000 mm^3, the tumor tissues were removed and divided. Then, the divided tissues were implanted into the underarm regions of 28 mice. Tumor sizes were determined through Vernier caliper measurements, and tumor volumes were calculated according to the formula: $(\text{shortest diameter})^2 \times (\text{longest diameter})/2$. When the tumor size reached approximately 100 mm^3, the mice were randomly divided into four groups (seven mice per group) for intraperitoneal injection (ip) daily with either: the vehicle control group, **25** 6.7 mg/kg treated group, **25** 20.0 mg/kg treated group, and the Cisplatin 1.0 mg/kg treated group (three weeks). The tumor size and body weight of mice were measured once in 2 days after treatment, and growth curves were plotted using average tumor volume within each experimental group. At the end of the observation period, the animals were euthanized by cervical dislocation, and the tumors and organs were removed and weighed. The rate of inhibition (IR) was calculated according to the formula: IR = (1 − Mean tumor weight of the experimental group/Mean tumor weight of the control group) × 100%.

Acknowledgements

We thank the National Natural Science Foundation of China (Grants 21472252, 81330077) and Natural Science Foundation of Guangdong Province (Grants 2017A030313089, 2017A030308003), and the Guangdong Provincial Key Laboratory of Construction Foundation (2017B030314030) for financial support of this study.

Appendix A. Supplementary material

Supplementary data to this article can be found online at https://doi.org/10.1016/j.bioorg.2018.12.020.

References

[1] C.Y. Lin, J. Loven, P.B. Rahl, R.M. Paranal, C.B. Burge, J.E. Bradner, T.I. Lee, R.A. Young, Transcriptional amplification in tumor cells with elevated c-Myc, Cell 151 (2012) 56–67.
[2] F.M. Cui, X.J. Sun, C.C. Huang, Q. Chen, Y.M. He, S.M. Zhang, H. Guan, M. Song, P.K. Zhou, J. Hou, Inhibition of c-Myc expression accounts for an increase in the number of multinucleated cells in human cervical epithelial cells, Oncol. Lett. 14 (2017) 2878–2886.
[3] F. Wang, D. Zhang, J. Mao, X.X. Ke, R. Zhang, C. Yin, N. Gao, H. Cui, Morusin inhibits cell proliferation and tumor growth by down-regulating c-Myc in human gastric cancer, Oncotarget 8 (2017) 57187–57200.
[4] L.M.S.R. Chi, V. Dang, Eileen Emison, Sunkyu Kim, Qing Li, Julia E. Prescott, Diane Wonsey, Karen Zeller, Function of the c-Myc oncogenic transcription factor, Exp. Cell Res. 253 (1999) 63–77.
[5] E.P. Wright, H.A. Day, A.M. Ibrahim, J. Kumar, L.J. Boswell, C. Huguin, C.E. Stevenson, K. Pors, Z.A. Waller, Mitoxantrone and analogues bind and stabilize i-motif forming DNA sequences, Sci. Rep. 6 (2016) 39456–39462.
[6] M.S. Dorasamy, B. Choudhary, K. Nellore, H. Subramanya, P.F. Wong, Dihydroorotate dehydrogenase inhibitors target c-Myc and arrest melanoma, myeloma and lymphoma cells at S-phase, J. Cancer 8 (2017) 3086–3098.
[7] E.T. Oh, C.W. Kim, H.G. Kim, J.S. Lee, H.J. Park, Brusatol-mediated inhibition of c-Myc increases HIF-1alpha degradation and causes cell death in colorectal cancer under hypoxia, Theranostics 7 (2017) 3415–3431.
[8] T. Akinyeke, S.J. Weber, A.T. Davenport, E.J. Baker, J.B. Daunais, J. Raber, Effects of alcohol on c-Myc protein in the brain, Behav. Brain Res. 320 (2017) 356–364.
[9] R.J. Floor, H.J. Wijma, P.A. Jekel, A.C. Terwisscha van Scheltinga, B.W. Dijkstra, D.B. Janssen, X-ray crystallographic validation of structure predictions used in computational design for protein stabilization, Proteins 83 (2015) 940–951.
[10] V. Gonzalez, L.H. Hurley, The c-MYC NHE III(1): function and regulation, Annu. Rev. Pharmacol. Toxicol. 50 (2010) 111–129.
[11] T.M. Ou, J. Lin, Y.J. Lu, J.Q. Hou, J.H. Tan, S.H. Chen, Z. Li, Y.P. Li, D. Li, L.Q. Gu, Z.S. Huang, Inhibition of cell proliferation by quindoline derivative (SYUIQ-05) through its preferential interaction with c-myc promoter G-quadruplex, J. Med. Chem. 54 (2011) 5671–5679.
[12] J. Ruan, T. Mouveaux, S.H. Light, G. Minasov, W.F. Anderson, S. Tomavo, H.M. Ngo, The structure of bradyzoite-specific enolase from Toxoplasma gondii reveals insights into its dual cytoplasmic and nuclear functions, Acta Crystallogr. D Biol. Crystallogr. 71 (2015) 417–426.
[13] B. Shu, J. Cao, G. Kuang, J. Qiu, M. Zhang, Y. Zhang, M. Wang, X. Li, S. Kang, T.M. Ou, J.H. Tan, Z.S. Huang, D. Li, Syntheses and evaluation of new acridone derivatives for selective binding of oncogene c-myc promoter i-motifs in gene transcriptional regulation, Chem. Commun. (Camb.) 54 (2018) 2036–2039.
[14] M. Debnath, S. Ghosh, A. Chauhan, R. Paul, K. Bhattacharyya, J. Dash, Preferential targeting of i-motifs and G-quadruplexes by small molecules, Chem. Sci. 8 (2017) 7448–7456.
[15] E.F. Michelotti, G.A. Michelotti, A.I. Aronsohn, D. Levens, Heterogeneous nuclear ribonucleoprotein K is a transcription factor, Mol. Cell. Biol. 16 (1996) 2350–2360.
[16] L. He, X. Xue, Z. Wang, E. Hou, Y. Liu, M. Liang, Y. Zhang, Z. Tian, Transcriptional regulation of heterogeneous nuclear ribonucleoprotein K gene expression, Biochimie 109 (2015) 27–35.
[17] L.C. Chen, H.P. Liu, H.P. Li, C. Hsueh, J.S. Yu, C.L. Liang, Y.S. Chang, Thymidine phosphorylase mRNA stability and protein levels are increased through ERK-mediated cytoplasmic accumulation of hnRNP K in nasopharyngeal carcinoma cells, Oncogene 28 (2009) 1904–1915.
[18] T. Tomonaga, D. Levens, Heterogeneous nuclear ribonucleoprotein K is a DNA-binding transactivator, J. Biol. Chem. 270 (1995) 4875–4881.
[19] D.J. Uribe, K. Guo, Y.J. Shin, D. Sun, Heterogeneous nuclear ribonucleoprotein K and nucleolin as transcriptional activators of the vascular endothelial growth factor promoter through interaction with secondary DNA structures, Biochemistry 50 (2011) 3796–3806.
[20] H.J. Kim, J.J. Lee, J.H. Cho, J. Jeong, A.Y. Park, W. Kang, K.J. Lee, Heterogeneous nuclear ribonucleoprotein K inhibits heat shock-induced transcriptional activity of heat shock factor 1, J. Biol. Chem. 292 (2017) 12801–12812.
[21] A.M.L. Vinicius Barreto da Silva, Carlton Anthony Taft, Carlos Henrique Tomich de Paula da Silva, Toxicophoric and metabolic in silico evaluation of benzimidazole and phenylbenzamide derivatives with potential application as anticancer agents, Drug Metab. Lett. 1 (2011) 267–275.

[22] M. Takimoto, T. Tomonaga, M. Matunis, M. Avigan, H. Krutzsch, G. Dreyfuss, D. Levens, Specific binding of heterogeneous ribonucleoprotein particle protein K to the human c-myc promoter, in vitro, J. Biol. Chem. 268 (1993) 18249–18258.
[23] C. Sutherland, Y. Cui, H. Mao, L.H. Hurley, A mechanosensor mechanism controls the G-Quadruplex/i-Motif molecular switch in the MYC promoter NHE III1, J. Am. Chem. Soc. 138 (2016) 14138–14151.
[24] D.S.a.L.H. Hurle, The importance of negative superhelicity in inducing the formation of G-Quadruplex and i-Motif structures in the c-Myc promoter: implications for drug targeting and control of gene expression, J. Med. Chem. 52 (2009) 2863–2874.
[25] T. Lemarteleur, D. Gomez, R. Paterski, E. Mandine, P. Mailliet, J.F. Riou, Stabilization of the c-myc gene promoter quadruplex by specific ligands' inhibitors of telomerase, Biochem. Biophys. Res. Commun. 323 (2004) 802–808.
[26] Z. Niknezhad, L. Hassani, D. Norouzi, Investigating actinomycin D binding to G-quadruplex, i-motif and double-stranded DNA in 27-nt segment of c-MYC gene promoter, Mater. Sci. Eng. C Mater. Biol. Appl. 58 (2016) 1188–1193.
[27] M. Zeraati, D.B. Langley, P. Schofield, A.L. Moye, R. Rouet, W.E. Hughes, T.M. Bryan, M.E. Dinger, D. Christ, I-motif DNA structures are formed in the nuclei of human cells, Nat. Chem. (2018).
[28] J. Strozynski, J. Heim, S. Bunbanjerdsuk, N. Wiesmann, L. Zografidou, S.K. Becker, A.M. Meierl, H. Gouveris, H. Luddens, F. Grus, J. Brieger, Proteomic identification of the heterogeneous nuclear ribonucleoprotein K as irradiation responsive protein related to migration, J. Proteomics 113 (2015) 154–161.
[29] R. Gao, N. Shah, J.S. Lee, S.P. Katiyar, L. Li, E. Oh, D. Sundar, C.O. Yun, R. Wadhwa, S.C. Kaul, Withanone-rich combination of Ashwagandha withanolides restricts metastasis and angiogenesis through hnRNP-K, Mol. Cancer Ther. 13 (2014) 2930–2940.
[30] L. Zhang, J. Feng, S. Kong, M. Wu, Z. Xi, B. Zhang, W. Fu, Y. Lao, H. Tan, H. Xu, Nujiangexathone A, a novel compound from Garcinia nujiangensis, suppresses cervical cancer growth by targeting hnRNPK, Cancer Lett. 380 (2016) 447–456.
[31] A.S.F. Matheus G. de Oliveira, Gilberto L.B. de Aquino, Andréia M. Leopoldino, Vinicius B. da Silva4, Carlton A. Taft and Carlos H.T. de Paula da Silva, In silico design of phenylbenzamide derivatives coupled to pyrimidines as novel hnRNP K ligands against cancer, Curr. Bioactive Compounds 10 (2014) 158–162.
[32] Q. He, P. Zeng, J.H. Tan, T.M. Ou, L.Q. Gu, Z.S. Huang, D. Li, G-quadruplex-mediated regulation of telomere binding protein POT1 gene expression, Biochim. Biophys. Acta, Mol. Cell. Biol. Lipids 2014 (1840) 2222–2233.
[33] J. Qiu, S. Chen, L. Su, J. Liu, N. Xiao, T.M. Ou, J.H. Tan, L.Q. Gu, Z.S. Huang, D. Li, Cellular nucleic acid binding protein suppresses tumor cell metastasis and induces tumor cell death by downregulating heterogeneous ribonucleoprotein K in fibrosarcoma cells, Biochim. Biophys. Acta, Mol. Cell. Biol. Lipids 2014 (1840) 2244–2252.
[34] P.H. Backe, A.C. Messias, R.B. Ravelli, M. Sattler, S. Cusack, X-ray crystallographic and NMR studies of the third KH domain of hnRNP K in complex with single-stranded nucleic acids, Structure 13 (2005) 1055–1067.
[35] Y.M. Yoga, D.A. Traore, M. Sidiqi, C. Szeto, N.R. Pendini, A. Barker, P.J. Leedman, J.A. Wilce, M.C. Wilce, Contribution of the first K-homology domain of poly(C)-binding protein 1 to its affinity and specificity for C-rich oligonucleotides, Nucl. Acids Res. 40 (2012) 5101–5114.
[36] T. Tomonaga, D. Levens, Activating transcription from single stranded DNA, Proc. Natl. Acad. Sci. USA 93 (1996) 5830–5835.
[37] D.T. Braddock, J.L. Baber, D. Levens, G.M. Clore, Molecular basis of sequence-specific single-stranded DNA recognition by KH domains: solution structure of a complex between hnRNP K KH3 and single-stranded DNA, EMBO J. 21 (2002) 3476–3485.
[38] J. Dai, E. Hatzakis, L.H. Hurley, D. Yang, I-motif structures formed in the human c-MYC promoter are highly dynamic–insights into sequence redundancy and I-motif stability, PLoS One 5 (2010) e11647.
[39] J.M. Dettler, R. Buscaglia, J. Cui, D. Cashman, M. Blynn, E.A. Lewis, Biophysical characterization of an ensemble of intramolecular i-motifs formed by the human c-MYC NHE III1 P1 promoter mutant sequence, Biophys. J. 99 (2010) 561–567.
[40] R.V. Brown, T. Wang, V.R. Chappeta, G. Wu, B. Onel, R. Chawla, H. Quijada, S.M. Camp, E.T. Chiang, Q.R. Lassiter, C. Lee, S. Phanse, M.A. Turnidge, P. Zhao, J.G.N. Garcia, V. Gokhale, D. Yang, L.H. Hurley, The consequences of overlapping G-Quadruplexes and i-Motifs in the platelet-derived growth factor receptor beta core promoter nuclease hypersensitive element can explain the unexpected effects of mutations and provide opportunities for selective targeting of both structures by small molecules to downregulate gene expression, J. Am. Chem. Soc. 139 (2017) 7456–7475.
[41] X. Li, Y. Peng, J. Ren, X. Qu, Carboxyl-modified single-walled carbon nanotubes selectively induce human telomeric i-motif formation, Proc. Natl. Acad. Sci. USA 103 (2006) 19658–19663.
[42] Y. Peng, X. Li, J. Ren, X. Qu, Single-walled carbon nanotubes binding to human telomeric i-motif DNA: significant acceleration of S1 nuclease cleavage rate, Chem. Commun. (Camb.) 5176–5178 (2007).
[43] C. Zhao, J. Ren, X. Qu, Single-walled carbon nanotubes binding to human telomeric i-motif DNA under molecular-crowding conditions: more water molecules released, Chemistry 14 (2008) 5435–5439.
[44] H.Y. Liu, A.C. Chen, Q.K. Yin, Z. Li, S.M. Huang, G. Du, J.H. He, L.P. Zan, S.K. Wang, Y.H. Xu, J.H. Tan, T.M. Ou, D. Li, L.Q. Gu, Z.S. Huang, New Disubstituted quindoline derivatives inhibiting Burkitt's lymphoma cell proliferation by impeding c-MYC transcription, J. Med. Chem. 60 (2017) 5438–5454.
[45] Y.Q. Wang, Z.L. Huang, S.B. Chen, C.X. Wang, C. Shan, Q.K. Yin, T.M. Ou, D. Li, L.Q. Gu, J.H. Tan, Z.S. Huang, Design, synthesis, and evaluation of new selective NM23-H2 binders as c-MYC transcription inhibitors via disruption of the NM23-H2/G-Quadruplex interaction, J. Med. Chem. 60 (2017) 6924–6941.
[46] M. Jerabek-Willemsen, C.J. Wienken, D. Braun, P. Baaske, S. Duhr, Molecular interaction studies using microscale thermophoresis, Assay Drug Dev. Technol. 9 (2011) 342–353.
[47] B.L. Staker, K. Hjerrild, M.D. Feese, C.A. Behnke, A.B. Burgin Jr., L. Stewart, The mechanism of topoisomerase I poisoning by a camptothecin analog, Proc Natl Acad Sci U S A 99 (2002) 15387–15392.
[48] T.Y. Hsu, L.M. Simon, N.J. Neill, R. Marcotte, A. Sayad, C.S. Bland, G.V. Echeverria, T. Sun, S.J. Kurley, S. Tyagi, K.L. Karlin, R. Dominguez-Vidana, J.D. Hartman, A. Renwick, K. Scorsone, R.J. Bernardi, S.O. Skinner, A. Jain, M. Orellana, C. Lagisetti, I. Golding, S.Y. Jung, J.R. Neilson, X.H. Zhang, T.A. Cooper, T.R. Webb, B.G. Neel, C.A. Shaw, T.F. Westbrook, The spliceosome is a therapeutic vulnerability in MYC-driven cancer, Nature 525 (2015) 384–388.
[49] B.J. Chen, Y.L. Wu, Y. Tanaka, W. Zhang, Small molecules targeting c-Myc oncogene: promising anti-cancer therapeutics, Int. J. Biol. Sci. 10 (2014) 1084–1096.
[50] P.D. Fahrlander, J. Sumegi, J.Q. Yang, F. Wiener, K.B. Marcu, G. Klein, Activation of the c-myc oncogene by the immunoglobulin heavy-chain gene enhancer after multiple switch region-mediated chromosome rearrangements in a murine plasmacytoma, Proc. Natl. Acad. Sci. USA 82 (1985) 3746–3750.
[51] K. Alitalo, M. Schwab, C.C. Lin, H.E. Varmus, J.M. Bishop, Homogeneously staining chromosomal regions contain amplified copies of an abundantly expressed cellular oncogene (c-myc) in malignant neuroendocrine cells from a human colon carcinoma, Proc. Natl. Acad. Sci. USA 80 (1983) 1707–1711.
[52] R. Gao, Y. Yu, A. Inoue, N. Widodo, S.C. Kaul, R. Wadhwa, Heterogeneous nuclear ribonucleoprotein K (hnRNP-K) promotes tumor metastasis by induction of genes involved in extracellular matrix, cell movement, and angiogenesis, J. Biol. Chem. 288 (2013) 15046–15056.
[53] A. Matta, S.C. Tripathi, L.V. DeSouza, J. Grigull, J. Kaur, S.S. Chauhan, A. Srivastava, A. Thakar, N.K. Shukla, R. Duggal, S. DattaGupta, R. Ralhan, K.W. Michael Siu, Heterogeneous ribonucleoprotein K is a marker of oral leukoplakia and correlates with poor prognosis of squamous cell carcinoma, Int. J. Cancer 125 (2009) 1398–1406.
[54] Z.Q. Zhou, P.J. Hurlin, The interplay between Mad and Myc in proliferation and differentiation, Trends Cell Biol. 11 (2001) 10–14.